

Ar-Ar and U-Pb Ages of Chelyabinsk and a Re-Evaluation of Its Impact Chronology

S.P. BEARD^{1,2,3,4*}, T.D. SWINDLE^{2,3}, T.J. LAPEN⁵, D.A. KRING^{2,6}. ¹State Key Laboratory in Lunar and Planetary Science, Macau University of Science and Technology, Avenida Wai Long, Taipa, 999078, Macau. ²NASA Solar System Exploration Research Virtual Institute, Moffett Field, CA 94035. ³Lunar and Planetary Laboratory, University of Arizona, Tucson AZ 85721, ⁴CNSA Macau Center for Space Exploration and Science, Macau, PR China. ⁵University of Houston, Houston TX 77004, ⁶Lunar and Planetary Institute, Houston TX 77058.

*Corresponding author. E-mail: spbeard@must.edu.mo

Abstract- The LL5 chondrite Chelyabinsk has had numerous isotopic studies since its fall in 2013. This data has been used to suggest ~8 impact events recorded from multiple isotopic systems (e.g., Ar-Ar, U-Pb, Sm-Nd, Rb-Sr, among others). We report details of Ar-Ar and U-Pb results and re-evaluate the geochronology of Chelyabinsk. Argon records the youngest Ar-Ar age recorded in meteorites, **25 ± 11 Ma**, and an older resetting event at **~2550 Ma**. The U-Pb analysis has an upper concordia age of **4456 ± 23 Ma** and a lower concordia age of **184 ± 200 Ma**. The lower concordia intercept represents a later thermal event (e.g., an impact), the most recent time that lead loss occurred, and could represent resetting by the youngest event recorded by Ar-Ar. Combining our data with literature results, we find strong evidence of at least four impact events (~4450, 2550, 1700, 25 Ma), with some evidence for two additional impacts (~3700, 1000 Ma).

INTRODUCTION

Chelyabinsk is an LL5 chondrite (Popova et al. 2013) that fell over the Chelyabinsk region of Russia in early 2013 (~500 kg TNT equivalent, Brown et al. 2013). The recovered samples are cross-cut with impact melt veins, presumably from older collisional events (Galimov et al. 2013, Badyukov et al. 2015), and have light-colored clast-rich and darker melt-rich lithologies (see supplementary figures). The clast-rich lithology is described as a typical chondritic texture of petrographic type 5, shock stage 4, and contains 1-2 mm thick melt veins (Badyukov et al. 2015). The dark melt-rich lithology contains impact melt that sometimes appears as dikes up to a few centimeters wide (Badyukov et al. 2015). Silicate minerals in Chelyabinsk are olivine, orthopyroxene, plagioclase, and clinopyroxene (decreasing order of abundance), and minor phosphate, ilmenite, troilite, chromite, and pentlandite. Metal phases include kamacite and taenite (Popova et al. 2013; Badyukov et al. 2015). Shock features include undulatory extinction and moderate to strong mosaicism in olivine and transformation of plagioclase into glass (Badyukov et al. 2015; Righter et al. 2015). The dark lithology is suggested to be the result of “shock darkening”, produced by a fine-grain redistribution of metal and sulfide-rich melt (Bischoff et al. 2013; Galimov et al. 2013, Righter et al. 2015), which may affect Ar-Ar dating results by altering minerals (Trieloff et al. 2018). The formation of the brecciated nature of Chelyabinsk is attributed to a single energetic impact event based on petrology (Badyukov et al. 2015; Petrova et al. 2016). Geochronology studies of Chelyabinsk, however, have determined multiple ages

(Table 1) that have been interpreted to represent at least eight impact events (Richter et al. 2015). Chelyabinsk is classified as shock S4 (Badyukov et al. 2015) and contains high-shock melt and low-shock clasts. This heterogeneity can add to the confusion when comparing different dating studies performed on melt, clasts, or mixtures. Keeping this in mind, Ar-Ar and U-Pb measurements of Chelyabinsk from this work will be described and combined with results from several other studies (Table 1) to suggest a scenario for the chronology of Chelyabinsk.

Table 1. Chelyabinsk ages determined by various isotopic dating methods.

Method	U-He	Ar-Ar	K-Ar	Rb-Sr	Sm-Nd	U-Pb and Pb-Pb	Re-Os
Age	~27 ²	25 ± 11 ¹	865 ± 97 ²	29 ± 54 ¹³	~290 ⁷	-9 ± 55 ^{11,14}	~4558 ¹²
		~30 ⁴	~1000 ⁵	880 ± 120 ²	2900 ± 500 ²	184 ± 200 ^{1,11}	
		312 ± 6 ^{2,3}	1945 ± 168 ²	1400 ± 300 ²	3733 ± 110 ⁸	834 ± 7 ⁹	
		716 ± 30 ²	1952 ± 169 ²	~4567 ⁶		2744 ± 13 ⁹	
		1014 ± 24 ^{2,3}	2736 ± 199 ²			2861 ± 15 ⁹	
		1184 ± 40 ^{2,3}				4433 ± 110 ¹⁰	
		1700 ± 100 ⁴				4456 ± 23 ^{1,11}	
		2544 ± 68 ¹				4461 ± 25 ¹	
						4473 ± 11 ^{11,14}	
						4538 ± 2 ¹¹	

1. This study, 2. Richter et al. (2015), 3. Lindsay et al. (2015), 4. Trierloff et al. (2017), 5. Haba et al. (2014), 6. Nakamura et al. (2015), 7. Galimov et al. (2013), 8. Bogomolov et al. (2015), 9. Skublov et al. (2015), 10. Kamioka et al. (2014), 11. Popova et al. (2013), 12. Day et al. (2014), 13. Nakamura et al. (2019), 14. Walton et al. 2022. All Ages are in Ma.

METHODS

Ar-Ar Analysis

Two Chelyabinsk samples, clast-rich MB020f,2 (MB,2) and melt-rich MB020f,5 (MB,5), were each divided into multiple aliquots, or splits, of ~10 to 14 mg for Ar-Ar analysis. The splits were irradiated at the Cadmium-Lined In-Core Irradiation Tube (CLICIT) facility at Oregon State University along with PP-20 Hb3gr Hornblende GSC (1081 ± 1.2 Ma, Renne et al. 2011) as the primary irradiation monitor to determine the J-factor, roughly 1.05×10⁻³ among our samples.

Samples were irradiated for four hours in the linear-with-height portion of the reactor to provide a more evenly distributed neutron flux. Samples were then allowed to cool for about two months to allow for short-lived isotopes to decay before being placed in a glass storage tree above a double-vacuum, resistance-heated furnace. The outer portion of the furnace is enveloped by a copper coil that contains chilled running water and is kept under a low vacuum (~10⁻³ torr) to reduce the amount of oxidation of the crucible. The inner portion of the tungsten furnace contains a tantalum crucible that has an opening in its base for inserting a tungsten-rhenium (W-Re) thermocouple, and it is in direct contact with the sample holder and the volume of the rest of the argon extraction line (~10⁻⁸ torr). Power to the furnace is supplied by a low-voltage, high-current Electronic Instruments (model TCR 10T500-1-D) transformer that is controlled by a WatLow PID (Proportional Integral

Derivative) temperature controller. Typical temperature steps were from 300 to 1500 °C in 25 to 200 °C intervals depending on the amount of argon released and the accuracy desired. The total number of heating steps varied between 16 and 32 per split. The temperature set point, opening and closing of valves, and mass spectrometer data collection were all automated and controlled by software developed by Alan Deino (Deino 2001).

The decay constants used are those reported in Renne et al. (2011). Corrections were applied to account for blanks, instrumental mass discrimination, spallation-produced isotopes, inherited/trapped argon, and interfering isotopes produced in the reactor from Ca and K. Isotopic measurements were regressed to a time of zero using linear regression techniques, after subtracting baseline values to get the most accurate measurements. Isochrons were determined by a least-squares method to provide the best fit (using source code by Philip Kromer based on Reed, 1989). This method determines the line that minimizes the distance between all the data weighed by the inverse square of the uncertainty in both the x and y direction.

Sample ages were determined based on ^{40}Ar - ^{39}Ar apparent age spectra (“plateau plots”). If the definition of a plateau as a region that contains at least 50% of the ^{39}Ar and at least three consecutive temperature steps that agree at a 95 % confidence level (Deino, 2001) is followed, then only one of the splits in this work has a plateau. However, there are “partial plateaus” that incorporate a smaller fraction of the total ^{39}Ar but contain the majority of the ^{39}Ar from the portion that has distinct K/Ca ratios. Ages for partial plateaus are given at the 2σ level and are calculated using the mean of all the steps in the plateau region, weighted by the amount of gas contained in each step. The K/Ca (see supplementary materials) released at successive temperatures behaves similarly to the K/Ca of Chelyabinsk samples analyzed by Trieloff et al. (2018).

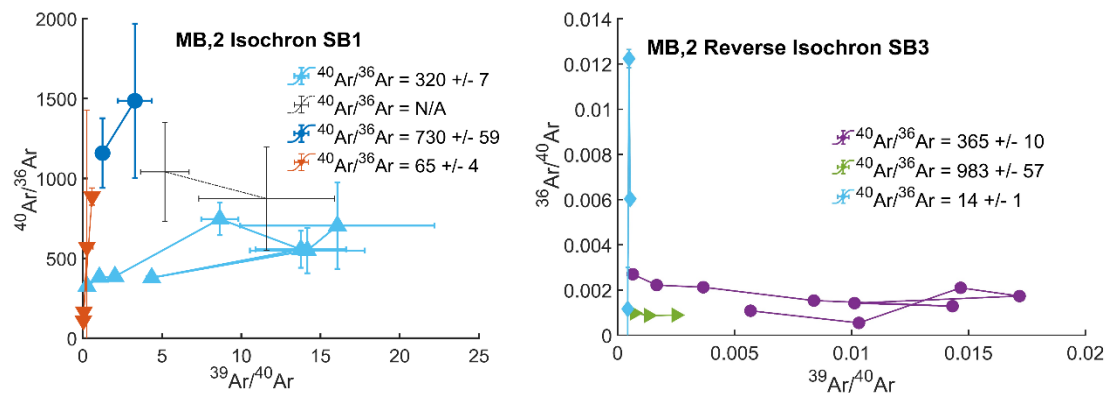


Figure 1. Example of isochron plots for 2 splits of MB,2 from Chelyabinsk. Both figures show the typical behavior of the trapped components observed in this sample (whether reverse or standard isochron format). Multiple trapped components were identified (plotted in different colors) using a least-squares fitting procedure that includes errors in both the x and y directions. Additional data are plotted in supplemental figures S3-S9. Colored figures can be found in the online version.

U-Pb/Pb-Pb Analysis

We analyzed U-Pb in phosphate minerals from a thick section made from a 4.84 g fragment labeled ‘C4’ of Popova et al. (2013). The specimen is from the clast-rich lithology that contains thin (10-20 μm wide) melt veins. For U-Pb analyses, phosphate grains were located and imaged with P, Ca, and Cl X-rays in maps of a roughly 1.5 by 2 mm portion

of the section surface. Two phosphate minerals are recognized; Cl-apatite and merrillite are randomly distributed across the sample area. The phosphates typically have irregular grain boundaries and range in size from a few microns to over 200 μm in diameter. The grains targeted for analyses are typically $> 50 \mu\text{m}$ in diameter.

In-situ U-Th-Pb isotope analyses of phosphates were conducted by LA-ICPMS at the University of Houston using a Varian 810 quadrupole ICPMS coupled with a Photon Machines Analyte.193 excimer laser ablation system. The laser ablation was performed using a 25 μm diameter circular laser spot with a 10 Hz repetition rate. Each analysis included measurement of a 'gas blank' for 20 seconds, followed by 24 seconds of sample ablation with a fluence of 3 J/cm^2 . Common Pb corrections were only applied to the calibration standards; common Pb contents in the samples were below instrument detection. Internal standards used to correct for instrumental mass and element fractionation are 958 ± 13 Ma grains (Thomson et al. 2012) from the Bear Lake region of the Bancroft terrane, Canada. Our external calibration standards were from Yates Mine, Otter Lake area, Canada. These were analyzed after four sample analyses. Results for the external standards yield a 944.3 ± 11 Ma U-Pb concordia age which agrees with an in-situ LA-ICPMS U-Pb age of 933 ± 12 Ma by Chew et al. (2011) but is older than a Pb-Pb step leaching age of 913 ± 7 Ma (Barfod et al. 2005).

Data reduction followed methods outlined in Shaulis et al. (2010; 2017) and Sarafian et al. (2017) and all uncertainties for the calibration standards were propagated into the uncertainties for sample data points. All uncertainties are reported at the 95% confidence interval.

RESULTS

Ar-Ar Results

Standard and reverse isochron plots (e.g., Fig. 1) were evaluated for the presence of trapped argon and they indicate multiple trapped components in both samples. MB020f,2 isochrons typically imply trapped $^{40}\text{Ar}/^{36}\text{Ar}$ ratios of ~ 300 to 400 for temperatures below ~ 600 to 700°C , a larger trapped $^{40}\text{Ar}/^{36}\text{Ar}$ component is found from intermediate temperature steps ($^{40}\text{Ar}/^{36}\text{Ar} \sim 730$ -1400, ~ 750 -1000 $^\circ\text{C}$), and a smaller trapped component at high temperature steps ($^{40}\text{Ar}/^{36}\text{Ar} \sim 14$ -132, ~ 1000 -1500 $^\circ\text{C}$).

The isochrons of MB020f,5 show similar behavior as those discussed for MB020f,2, but generally indicate lower $^{40}\text{Ar}/^{36}\text{Ar}$ trapped components. Low temperature data indicate a trapped $^{40}\text{Ar}/^{36}\text{Ar} \sim 211$ -283 (~ 300 -650 $^\circ\text{C}$), intermediate temperatures have $^{40}\text{Ar}/^{36}\text{Ar} = 320$ -1235 (~ 600 -1200 $^\circ\text{C}$), and high temperatures indicate trapped $^{40}\text{Ar}/^{36}\text{Ar} = 34$ -808 (900-1500 $^\circ\text{C}$). The isochron ages of the splits are similar, despite the different trapped corrections (Table 2). Splits SB5 and CH2 both need an additional trapped correction that corresponds to the intermediate temperature steps, such a correction is not necessary for SB4.

Some isochron data from both samples do not behave well and no proper trapped correction can be identified (no correction of $^{40}\text{Ar}/^{36}\text{Ar}$ was applied to the corresponding steps, which are labeled as "N/A" in tables and figures). These data are strongly affected by a resetting event, and the choice of the correction value does not affect the overall results. A summary of the isochrons is shown in Table 2.

The apparent age/plateau plots for each set of splits from a single sample look very similar to one another but vary significantly from one sample to the other. The four splits (SB1, SB2, SB3, and CH1) of the clast rich (“light lithology”) MB020f,2 have low apparent ages for the first ~85% of the total ^{39}Ar released, before increasing, typically to ~2000 to 3000 Ma, in the highest-temperature extractions. Three of the splits give a series of concordant ages from about 40 to 50% of the ^{39}Ar released with an age of **25.0 ± 11.2 Ma**, which represents the best age for MB020f,2.

Much of the gas was released at low temperature steps, and consequently, the number of temperature steps was modified from 16 to 32 to better determine the age. The following results from MB020f,2 are presented in order of the split name.

SB1: The apparent age spectra of SB1 has a partial plateau of 29.8 ± 5.9 Ma (three temperature steps 450 to 550°C), containing ~40% of the released ^{39}Ar (Fig. 2). This partial plateau also corresponds to the minimum age observed. More details of each split can be found in the supplementary materials section.

SB2: It was not known beforehand which temperatures would correspond to the majority of the released argon. For the first analysis of a sample, we use a typical heating assignment that anticipates that most of the argon is released at intermediate temperatures. The first Chelyabinsk sample measured was SB2, which was analyzed with the typical heating schedule that proved to not be ideal; most of the gas was released at lower temperatures than expected. In the apparent age plot, there are two steps that contain 52% of the released ^{39}Ar and have a weighted age of 26.9 ± 10.2 Ma.

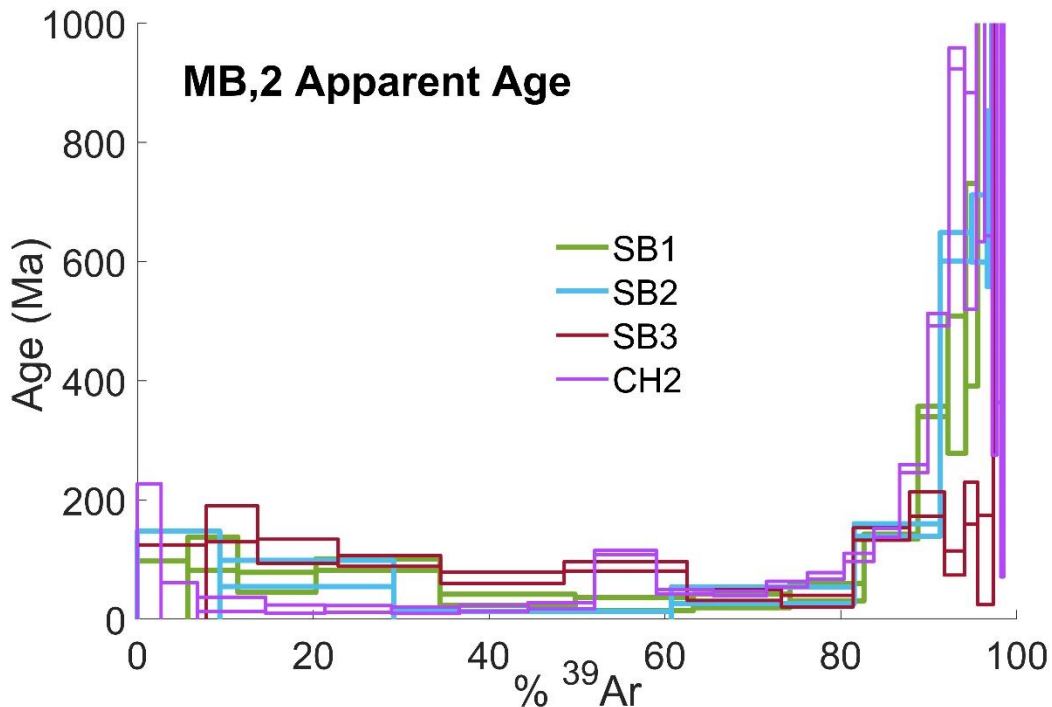


Figure 2. The average of the three splits that agreed (SB1, SB2, and CH1) within the standard deviation for the uncertainty results in **25.0 ± 11.2 Ma**. This age represents the upper age estimate for the most recent resetting impact event. Additional data are plotted in supplemental figures S3-S9. Colored figures can be found in the online version.

Table 2. Trapped Corrections and Isochron Ages for Chelyabinsk.

Sample	Split ID	Temp. (°C)	$^{40}\text{Ar}/^{36}\text{Ar}_{\text{Trapped}}$	Isochron Age (Ma)
MB020f,2 Clast Rich	SB1	250-600	320 ± 7	46 ± 11
		650-700	N/A	
		750-800	730 ± 59	
		1000-1500	65 ± 4	
	SB2	300-700	401 ± 25	19 ± 21
		800-950	1407 ± 160	
		975-1500	45 ± 40	
	SB3	250-700	365 ± 10	88 ± 19
		750-1000	983 ± 57	
		1200-1500	14 ± 1	
	CH1	250-300	323 ± 38	19 ± 8
		350-475	82 ± 22	
		500-800	N/A	
		850-1025	838 ± 52	
		1050-1500	132 ± 20	
MB020f,5 Melt Rich	SB4	400-600	243 ± 37	2276 ± 1315
		700-900	N/A	
		925-1075	323 ± 38	
		1100-1500	117 ± 56	
	SB5	300-500	283 ± 6	2612 ± 464
		600-800	800 ± 417	
		950-1200	688 ± 142	
		1225-1300	34 ± 29	
		1350-1500	268 ± 20	
	CH2	300-650	211 ± 10	2494 ± 538
		700-900	1235 ± 275	
		925-950	N/A	
950-1100		808 ± 172		
		1150-1500	220 ± 100	

SB3: This split has slightly higher ages than the other three splits and is generally more disturbed in appearance. Almost 40% of the gas was released in 3 steps from 400 to 500 °C with an age of 86.0 ± 5.0 Ma. However, we do not quote this as a best age since the steps disagree with the other three splits of the sample. It is possible that a portion of this split was not degassed as thoroughly as the others in the resetting event. The minimum age is similar to the minimum ages of the other splits (30.4 ± 9.7 Ma).

CH1: The split with the most heating steps, CH1, has a partial plateau of 18.2 ± 2.4 Ma, representing about 37% of the ^{39}Ar (375 to 475 °C). When determining our best age of the overall sample (Fig. 2), the average of the three splits that agree (SB1, SB2, and CH1) are used along with standard error propagation, which results in **25.0 ± 6.2 Ma**. This represents the upper limit to the age of the most recent impact event.

None of the splits from the melt rich MB020f,5 have apparent ages as low as the partial plateaus of the clast-rich splits. The high temperature steps have apparent ages as high as 3492 ± 135 Ma, which represents a lower limit of a possible relict impact age. The average of the plateau age from split CH2 with the partial plateaus from the other splits yields an age of **2544 ± 68 Ma**. The ages of each split are summarized in Table 3. The following discusses each split of the melt rich sample MB020f,5 separately.

SB4: The plateau plot of this split has a minimum age of 489 ± 23 Ma, followed by a stair-step pattern that ends with a series of similar ages at 2504 ± 26 Ma (5 steps, 975 to 1075°C, 22% of released ^{39}Ar).

SB5: The same pattern is seen in this sample, which has a minimum age of 697 ± 30 Ma. There is a series of similar ages at 2622 ± 34 Ma (7 steps, 1000 to 1200°C, 41% of the released ^{39}Ar). SB5 might also show evidence of a relict age of 3429 ± 99 Ma (3 concordant steps from 1225-1300°C).

CH2: The plateau plot of CH2 is similar to the other two splits. It has a minimum age of 698 ± 35 Ma, and a much broader plateau of high ages at 2506 ± 30 Ma (10 steps, 975 to 1400°C, 57% of the released ^{39}Ar). The apparent age spectra are summarized in Figure 3, with more detailed information that can be found in the supplementary material.

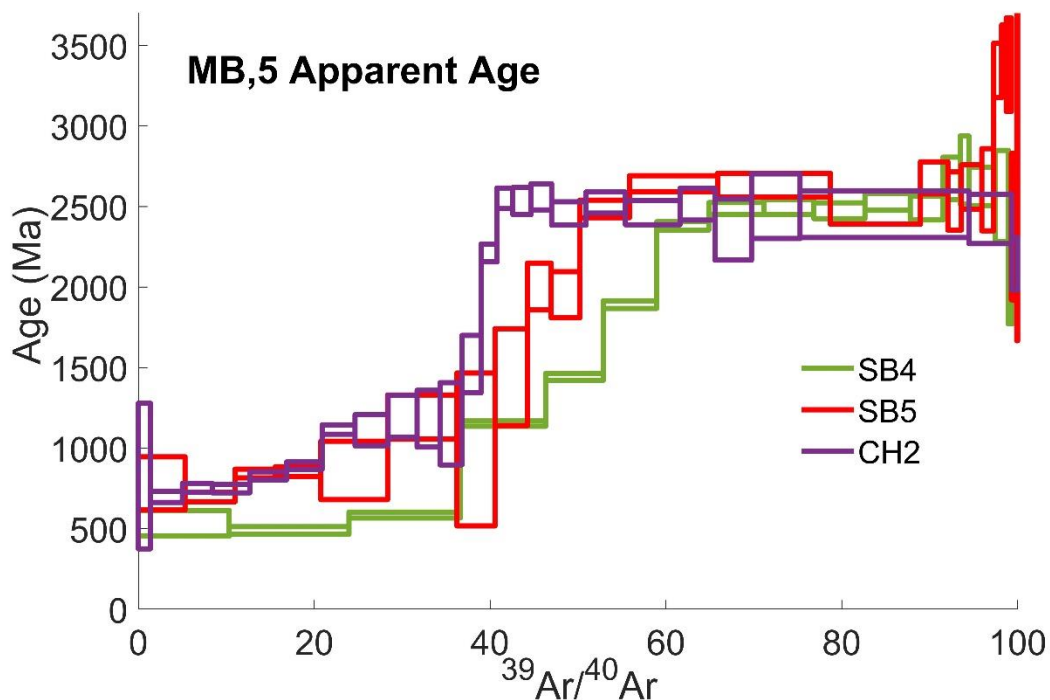


Figure 3. Apparent age spectra for all splits of melt-rich sample MB020f,5 (SB4, SB5, and CH2) show a diffusion pattern at low temperatures. The average age of the plateau and of partial plateaus is **2544 ± 68 Ma**. This is the best age estimate for a resetting impact event. Additional data are plotted in supplemental figures S3-S9. Colored figures can be found in the online version.

Table 3. Chelyabinsk Argon-Argon Age Summary.

Sample	Split ID	Min Age	Total Age	Plateau Age	# Steps	% ³⁹ Ar	Best age
MBO20F,2							25.0 ± 11.2
Clast Rich	SB1	25.4 ± 10.7	191.4 ± 6.7	(29.8 ± 5.9)	3	40	
	SB2	12.3 ± 14.8	213.6 ± 15.3	(26.9 ± 10.2)	2	52	
	SB3	30.4 ± 9.7	169.3 ± 7.3	(86.0 ± 5.0)	4	40	
	CH1	15.0 ± 5.4	185.6 ± 15.9	(18.2 ± 2.4)	5	37	
MBO20F,5						2544.4 ± 67.5	
Melt Rich	SB4	488.8 ± 23.4	1730.5 ± 15.9	(2504.3 ± 25.8)	4	22	
	SB5	697.4 ± 29.8	2035.0 ± 29.4	(2622.3 ± 33.7)	7	41	
	CH2	697.8 ± 34.7	2047.1 ± 42.1	2506.7 ± 29.4	10	57	

Partial plateaus are reported in parenthesis (#####). "Min" stands for minimum. All ages are in Ma. Best age for MB2 is determined from only SB1, SB2, and CH1 splits.

U-Pb and Pb-Pb Results

We analyzed 14 spots from 8 phosphate grains. Three of the grains were merrillite, and these did not have high enough U concentrations for age determinations. The remaining 5 grains (grains 1, 3, 4, 6, and 7; Table 4) were Cl-apatite. The Cl-apatite yielded a discordia line on a U-Pb concordia diagram with upper and lower intercept ages of 4477 ± 73 and 314 ± 470 Ma, respectively (Fig. 4). A weighted average $^{207}\text{Pb}/^{206}\text{Pb}$ age is 4461 ± 25 Ma ($n = 9$). The discordia line is unlikely related to residual instrumental elemental fractionation, as we did not observe residual elemental fractionation in the external apatite standards analyzed with the samples. Thus, we interpret the discordant data to be resulting from partial Pb-loss that happened relatively recently.

The U-Pb data presented here is considered in concert with U-Pb data of Popova et al. (2013), which yield identical concordia diagram intercepts within error. Figure 4 shows the collinearity of the data on a U-Pb concordia diagram where the upper and lower intercepts are 4456 ± 23 and 184 ± 200 , respectively, for the pooled data.

Table 4. U-Pb isotope compositions of chlorapatite minerals in Chelyabinsk.

Analysis_#	²⁰⁴ Pb/ ²⁰⁶ Pb	2SD	²⁰⁷ Pb/ ²⁰⁶ Pb	2SD	²⁰⁷ Pb/ ²³⁵ U	2SD	²⁰⁶ Pb/ ²³⁸ U	2SD	rho
Phos 1-1	0.0021	0.0040	0.574	0.019	53.7	2.4	0.683	0.024	0.74
Phos 1-2	-0.0031	0.0110	0.582	0.015	68.4	2.4	0.861	0.025	0.77
Phos 1-3	0.0015	0.0036	0.570	0.017	50.1	2.0	0.643	0.020	0.75
Phos 1-4	-0.0054	0.0060	0.586	0.016	54.3	2.0	0.676	0.021	0.77
Phos 1-5	0.0023	0.0082	0.592	0.016	42.5	1.5	0.558	0.017	0.77
Phos 3-1	0.0010	0.0025	0.562	0.016	51.4	1.8	0.635	0.018	0.70
Phos 4-1	0.0079	0.0088	0.567	0.017	46.2	1.9	0.602	0.020	0.77
Phos 6-1	0.0087	0.0209	0.598	0.019	50.5	2.1	0.620	0.020	0.73
Phos 7-1	0.0068	0.0076	0.597	0.019	40.2	2.0	0.515	0.023	0.85

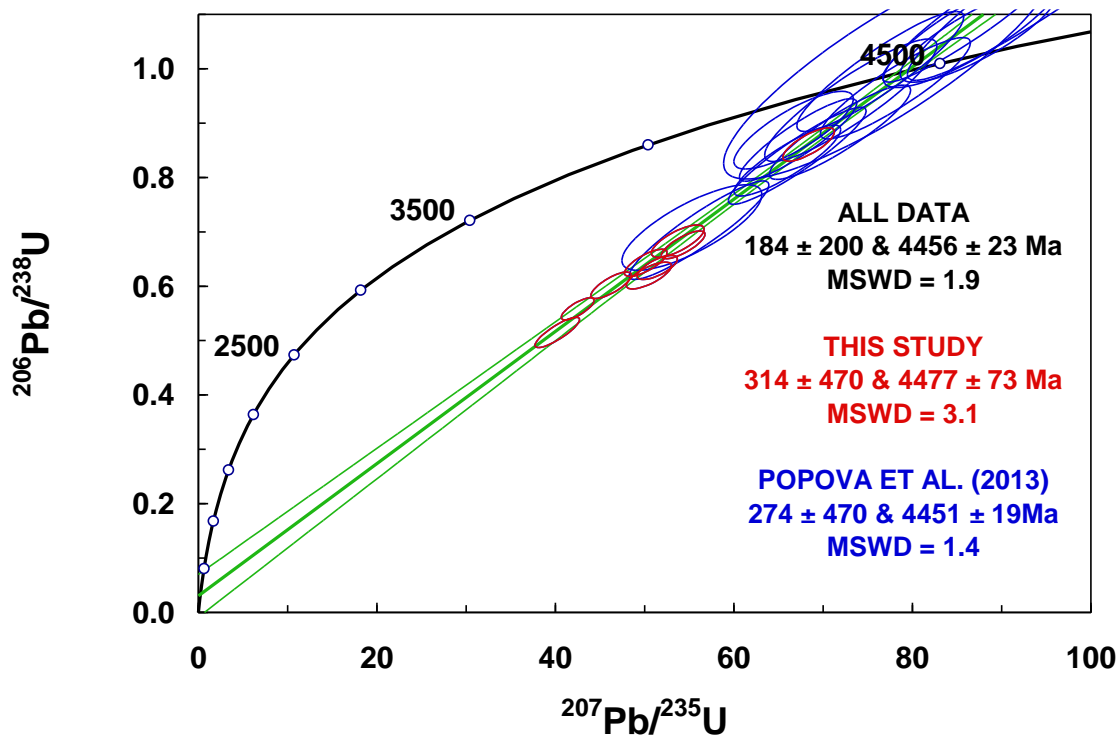


Figure 4. U-Pb concordia diagram of Chelyabinsk samples studied in this work (red ellipses) and from Popova et al. (2013) (blue ellipses). The combined data shows the collinearity of the data where the upper and lower intercepts are 4456 ± 23 Ma and 184 ± 200 Ma, respectively. Colored figures can be found in the online version.

IMPACT DISCUSSION

A brief qualitative description of the geochronology of Chelyabinsk, along with a relative level of confidence, is listed in Table 5. Generally speaking, a result has a high level of confidence if the quality of the data is high (there are multiple data points in an isochron or plateau, relatively low errors, clear reasoning for data point inclusion) and/or is consistent with results from other work (either from the same or different isotopic systems).

Ar-Ar

This work shows evidence of a recent impact event in Chelyabinsk MB020f,2 at 25.0 ± 11.2 Ma, which is significantly younger than such events for other known LL chondrites. Most LL chondrites have impact ages of 4200 to 4350 Ma (Swindle et al. 2014) with very few examples of resetting in the last 1500 Ma. The youngest $^{40}\text{Ar}/^{39}\text{Ar}$ ages are for the LL impact melts (LLIM) Yamato-790964 (1260 ± 24 , Takagami and Kaneoka 1987), NWA 1701 (970 ± 80 , Swindle et al. 2006), and LAR 06298/9 with an $^{40}\text{Ar}/^{39}\text{Ar}$ age of 200 ± 200 (Weirich et al. 2009; Swindle et al. 2011) and for the LL6 Morokweng fossil meteorite (625 ± 163 , Jourdan et al. 2010).

The clast-rich sample MB020f,2 yields younger apparent ages than the melt-rich sample, indicating that the clast was more thoroughly degassed than the melt in the most

recent event. Although this seems counterintuitive, this is not an unusual behavior (McConville et al. 1988; Bogard et al. 1995). The diffusional path length of argon in a clast is much shorter than the path length required to diffuse out of a melt. As such, a clast-rich sample's argon is more easily lost. Work by Trieloff et al. (2018) confirms lower ages in the clast-rich lithology (indistinguishable from the results in this work, ~30 Ma) and they explain the high retention of the melt material as a consequence of the formation of high-pressure phases of plagioclase as a result of shock metamorphism. One might consider that the clast-rich sample's young apparent age is a result of heating during Chelyabinsk's entry in the atmosphere and subsequent explosion. However, to drop the apparent age to 30 Ma from 4000 Ma would require that 99.8% of the argon to be degassed, and there is no evidence seen in the petrography for such extreme heating, which would be from the outside in. Therefore, we propose that the clast-rich sample's age of 25.0 ± 11.2 Ma does in fact represent an upper limit to the most recent Ar-Ar resetting impact.

The melt rich MB020f,5 sample shows minimum ages of ~490 Ma and has a partial plateau age of 2544.4 ± 67.5 Ma. This partial plateau age is consistent with Sm-Nd ages (Righter et al. 2015) of Chelyabinsk and is interpreted to represent a unique impact event not seen in other LL chondrites. Trieloff et al. (2018) studied dark lithologies and melt from Chelyabinsk and obtained different results (~1.7 Ga compared to ~2.5 Ga in this work). The shape of their age spectra are very reminiscent of the age spectra of MB020f,5. Using the model from Swindle and Weirich (2017), preliminary investigations as to whether or not this could be the result of the same event but with different physical conditions (temperature and duration of heating that could degas a sample more thoroughly) indicate that the results of Trieloff et al. (2018) and this work are unique impact events (see supplementary material).

U-Pb

Previous U-Pb chronologic studies of this meteorite include Pb-Pb step-leaching experiments of the dark impact-melt breccia lithology that yield an age of 4538.3 ± 2.1 Ma (Bouvier et al. 2013), which is one of the oldest ages determined for this meteorite. In-situ SIMS U-Pb analyses of phosphates from the melt breccia lithology yield an upper intercept on a concordia diagram of 4452 ± 21 Ma (Popova et al. 2013) (Fig. 4) and an age of 4433 ± 110 Ma (Kaminoka et al. 2014). The data of Popova et al. (2013), however, do not show evidence of extensive Pb-loss in phosphate as observed in our study. Recent work from Walton et al. (2022) targeted phosphate grains in light and dark lithologies, that combined with data from Popova et al. (2013), result in an upper intercept U-Pb age of 4473 ± 11 Ma and a lower intercept at -9 ± 55 Ma, which is consistent with our results.

The combined U-Pb data from this study and those of Popova et al. (2013) yield an upper intercept age of 4456 ± 23 Ma for both the chondrite and impact-melt breccia lithologies. As noted by those authors, these ages are younger than phosphate ages from other ordinary chondrites. This age is also younger than the Pb-Pb step leaching age from Bouvier et al. (2013), but it is difficult to compare these data because the in-situ technique targets single phases whereas the step-leaching technique analyzes mixtures of phases and their leachates. The upper intercept age of Fig. 4 most likely represents an early event that essentially reset the U-Pb isotope systematics of apatite and likely represents the timing of formation for the impact-melt breccia lithology. The lower intercept age of 184 ± 200 Ma (consistent with the U-Pb age of -9 ± 55 Ma, Walton et al. 2022) likely represents a late

thermal event that is also seen in the Sm-Nd, Rb-Sr, and Ar-Ar isotope systematics (Galimov et al. 2013, Nakamura et al. 2019, this work). Of note, the U-Pb data of this study from apatite in the clast-rich lithology exhibits a greater degree of Pb-loss than data obtained from the impact melt-rich lithology, consistent with observations of Ar loss from the different respective lithologies in Chelyabinsk.

Like the U-Pb lower concordia age, the Sm-Nd 'age' of ~290 Ma (Galimov et al. 2013) is consistent with our lower intercept age and may be a function of re-distribution of REE by phosphate mineral recrystallization/reaction during the late shock/heating event. The Ar-Ar age of 25 ± 11 Ma for the chondrite-textured lithology is likely the best estimate for the age of this event (Walton et al. 2022).

U-Pb ages from zircons are intermediate to the upper and lower concordia intercepts of apatite grains ($\sim 2850 \pm 15$ Ma and $\sim 840 \pm 10$ Ma, Skublov et al. 2015) of Chelyabinsk. Zircon has a much higher closure temperature than apatite ($\sim 500^\circ\text{C}$ for apatite, $> 1000^\circ\text{C}$ for zircon; Cherniak et al. 1991), making it unclear why the apatite grains were not also reset. Shock and heat experiments (Gaffney et al. 2011) show that Pb-Pb and U-Pb isochrons are generally affected, however it is not clear how the behavior of these systems change based on the target mineral. It seems reasonable that the upper concordia intercept of zircon should be older than the upper concordia intercept of apatite based on closure temperatures, but apatite is ~2 Ga older. Some possible explanations include a local difference recorded by the respective samples, shock effects, and unknown experimental error. However, recrystallization of zircon would require a non-local event that would be recorded in multiple chronometric systems. Perhaps the zircon components (Skublov et al. 2015) experienced an intense heating event, likely somewhere on the same parent body as Chelyabinsk, and were later transported/incorporated into the proto-Chelyabinsk mass before it broke off from the parent body. Another possibility is that there is an experimental artifact, which would most likely affect the zircon U-Pb ages; data come from only one study while the apatite ages have been independently verified (this work; Popova et al. 2013; Kamioka et al. 2014).

Sm-Nd

Three studies of Sm-Nd yield four very different ages; ~290, 2900 ± 500 , $\sim 3730 \pm 110$, and 4452 ± 21 Ma (Galimov et al. 2013; Righter et al. 2015; Bogomolov et al. 2013; and Righter et al. 2015, respectively). The Sm-Nd age of 290 Ma comes from unidentified rock separates, whole rock measurements, glass, and is the result of an isochron that is mostly defined by two samples (see Righter et al. 2015) and is difficult to interpret. If real, this would imply a high energy impact that would likely reset at least the Ar-Ar ages if not others. Alternatively, it could be the result of a re-distribution of REE as mentioned in the previous section. Furthermore, a 25 Ma age is not inconsistent with the data from Righter et al. (2015). A Sm-Nd age of 2900 ± 500 Ma is indistinguishable from the Ar-Ar age of MB0202f,5 in this work. This Sm-Nd age (2900 ± 500 Ma) is determined from removal (whole rock, magnetic separate) and addition (glass, whole rock, and non-magnetic separate) in measurements by Galimov et al. 2013 that is combined with one dark impact melt breccia measurement from Righter et al. (2015). Though the justification for addition and removal of measurements is not well explained, it is possible that this represents an energetic impact. The ~3700 Ma age is determined by data from three mineral separates that have had the data for the bulk rock measurement removed (Bogomolov et al. 2013).

The authors of that work note that if the bulk rock was included, the isochron represents an age ~ 700 Ma younger, which would be indistinguishable from the 2900 ± 500 Ma age reported in Richter et al. (2015) and may therefore represent the same event. The oldest Sm-Nd age of ~ 4452 Ma comes from only two whole rock (light lithology and light lithology that has been darkened by shock) measurements and is consistent with U-Pb and Pb-Pb results.

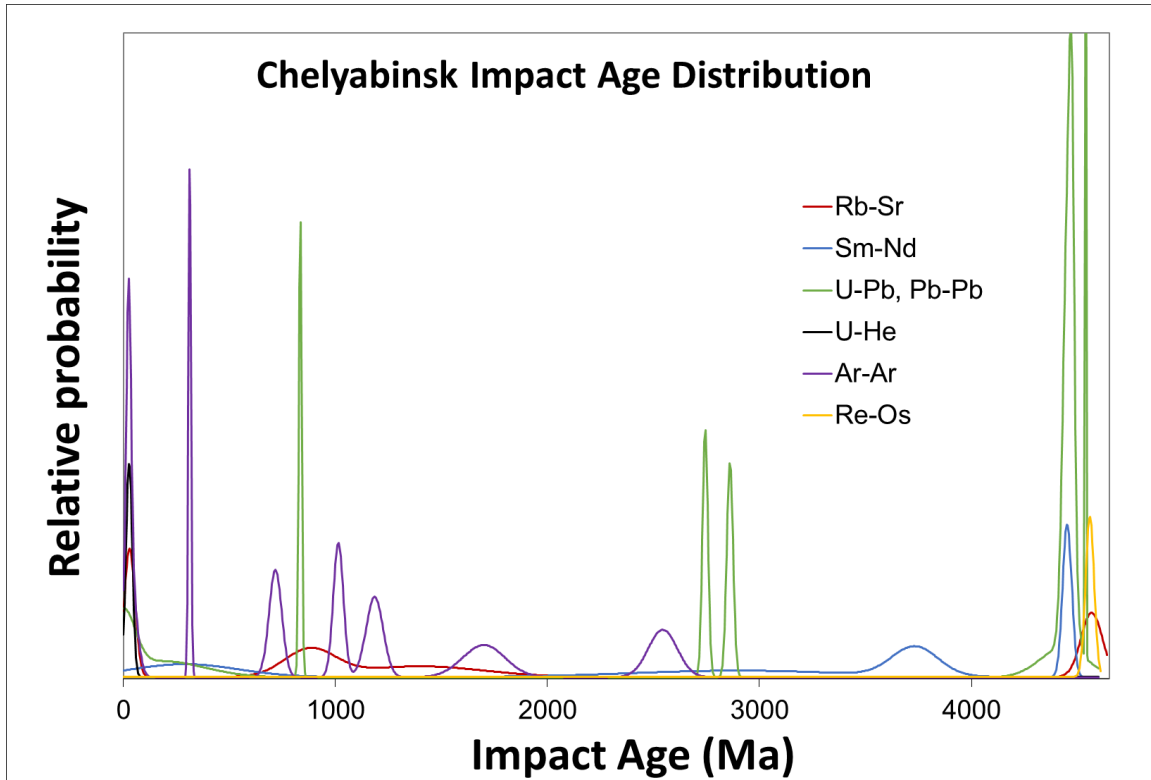


Figure 5. Revised impact age distribution suggested by this work. Formation age ~ 4560 Ma (Re-Os, Rb-Sr), an early energetic impact ~ 4450 Ma (Pb-Pb, U-Pb), an energetic impact not seen in other LL chondrites at ~ 2500 - 2800 Ma (Sm-Nd, U-Pb, Ar-Ar), followed by the most recent impact event ~ 30 Ma (Rb-Sr, U-He, U-Pb, Sm-Nd, and Ar-Ar). Based on quality and context of data, there is also possible evidence of an impact at ~ 3700 Ma (Sm-Nd) and at ~ 1000 Ma (Ar-Ar, Rb-Sr). See Table 5 for all references. Colored figures can be found in the online version. See Table 5 for references.

Rb-Sr

The Rb-Sr data for Chelyabinsk are also generally disturbed and difficult to interpret. Combined Rb-Sr literature data in Richter et al. (2015) show an isochron age of ~ 300 Ma, and they demonstrate that it is not distinguishable from an isochron age of ~ 30 Ma (which was included in their demonstration for comparison to early results of this work). In total they find two ages at 880 ± 120 and 1400 ± 300 Ma (Richter et al. 2015) that are defined by two data points and that are difficult to interpret. Nakamura et al. (2019) determined a well-defined 're-processed' Rb-Sr age of 29 ± 25 Ma from glass, which could represent the same impact event recorded in the Ar-Ar system (and probably U-Pb and Sm-Nd) of MB020f,2 at ~ 25 Ma.

Table 5. Summary of Chelyabinsk Ages.

Isotopes	Age (Ma)	Confidence	Notes
Ar-Ar	25 ± 11¹	H	Recent well-defined impact event measured from whole-rock in this work, agrees with Rb-Sr, U-He and consistent with U-Pb and Sm-Nd
	~ 30 ± 30 ³	H	Recent well-defined impact event in agreement with this work, Rb-Sr, U-He, consistent with U-Pb and Sm-Nd
	312 ± 6 ^{2,4}	L	"mixed-mostly light" lithology, moderately defined, consistent with U-Pb and Sm-Nd
	716 ± 30 ⁴	L	"mixed-mostly light" lithology, well defined, younger than but consistent with Rb-Sr
	1014 ± 24 ^{2,4}	I	Plagioclase separate from dark lithology, moderately defined
	1184 ± 40 ^{2,4}	I	Plagioclase separate from light lithology, well defined, consistent with Rb-Sr
	1700 ± 100 ³	H	Intermediate age from dark lithology, consistent with Rb-Sr, well defined
	2544 ± 68¹	H	Oldest argon 'plateau', from whole-rock dark lithology, measured in this work, consistent with Sm-Nd and U-Pb
K-Ar	865 ± 97 ⁴	VL	K-Ar is not appropriate for measuring multiple events*
	1000 ⁵	VL	K-Ar is not appropriate for measuring multiple events*
	1945 ± 168 ⁴	VL	K-Ar is not appropriate for measuring multiple events*
	1952 ± 169 ⁴	VL	K-Ar is not appropriate for measuring multiple events*
	2736 ± 199 ⁴	VL	K-Ar is not appropriate for measuring multiple events*
Rb-Sr	29 ± 54 ¹⁴	H	Agrees with Ar-Ar, U-He, and consistent with U-Pb and Sm-Nd, well-defined isochron
	880 ± 120 ⁴	I/L	Agrees with U-Pb, consistent with Ar-Ar, moderately/poorly defined
	1400 ± 300 ⁴	I/L	Consistent with Ar-Ar, moderately/poorly defined
Sr-Sr	4567 ⁶	L	Consistent with Pb-Pb and Re-Os but poorly defined
Sm-Nd	~290 ⁷	L	Consistent with U-Pb, Sm-Nd, and Ar-Ar, poorly defined
	2900 ± 500 ⁴	I/L	Consistent with Ar-Ar, moderately/poorly defined
	3733 ± 110 ⁸	I/L	Moderately-well defined, authors note that it could represent an event ~700 Ma younger
	4452 ± 21 ⁴	I	Consistent with U-Pb, Pb-Pb, moderately defined
U-Pb	-9 ± 55 ^{11,15}		Youngest evidence of lead loss, well defined, consistent with Ar-Ar, Rb-Sr, Sm-Nd, and other U-Pb results
	314 ± 470¹	I	Youngest evidence of lead loss, moderately defined, measured in this work, consistent with Ar-Ar, Rb-Sr, Sm-Nd, and U-Pb
	274 ± 470 ¹¹	I	Youngest evidence of lead loss, moderately defined, consistent with Ar-Ar, Rb-Sr, Sm-Nd, and this work
	834 ± 7 ⁹	I	Relatively young age from zircons that may represent impact elsewhere on parent body, well defined, agrees with Rb-Sr
	2744 ± 13 ⁹	I	Relatively young age from zircons that may represent impact elsewhere on parent body, well defined, older but consistent with Ar-Ar
	2861 ± 15 ⁹	I	Relatively young age from zircons that may represent impact elsewhere on parent body, well defined, older but consistent with Ar-Ar
	4433 ± 110 ¹⁰	I	Consistent with other U-Pb results
	4451 ± 19 ¹¹	H	Well defined, agrees with this work, Pb-Pb, and Sm-Nd
	4473 ± 11 ^{11,15}	H	Well defined, agrees with this work, Pb-Pb, and Sm-Nd
	4477 ± 73¹	H	Well defined, agrees with other U-Pb results, Pb-Pb, and Sm-Nd
	Pb-Pb	4538 ± 2 ¹²	H
4461 ± 25¹		H	Well defined, agrees with Sm-Nd
Re-Os	4558 ¹³	I	Consistent with Pb-Pb and Rb-Sr
U-He	~27 ²	I	Agrees with Ar-Ar, consistent with Rb-Sr, Sm-Nd, and U-Pb

*Indicates inclusion/exclusion in age distribution does not change results. ¹Indicates the K-Ar age agrees with the summed age of the Ar-Ar measurements from the melt-rich sample in this work. Bold ages are results from this work, bold descriptions are for unreliable measurements not included in Fig. 5. Confidence levels are designated as High (H), Intermediate (I), Low (L), and Very Low (VL) based on the quality of the plateau/isochron (number and quality of data points, justification for removal or inclusion) and agreement/consistency with results from other works. 1. This study, 2. Lindsay et al. (2015), 3. Trierloff et al. (2015), 4. Righter et al. (2015), 5. Haba et al. (2014), 6. Nakamura et al. (2015), 7. Galimov et al. (2013), 8. Bogomolov et al. (2013), 9. Skublov et al. (2015), 10. Kamioka et al. (2014), 11. Popova et al. (2013), 12. Bouvier (2013), 13. Day et al. (2014), 14. Nakamura et al. (2019), 15. Walton et al. (2022).

Age synthesis

It is difficult to explain every isochron age in a chronologically complex meteorite such as Chelyabinsk. The disturbed isochron plots for Sm-Nd and Rb-Sr are likely the result of shock effects and re-distribution of REE that make it difficult to determine a reliable age. However, with additional comparison to other chronometers, some of the Sm-Nd and Rb-Sr ages may have significant value.

The Pb-Pb and U-Pb ages are comparable to one another yet are much older than both the Ar-Ar and some of the Sm-Nd ages, which at first seems puzzling – since Pb-Pb generally resets more easily than Sm-Nd, and not as easily as Ar-Ar. We would therefore expect the age of Sm-Nd > Pb-Pb > Ar-Ar. Part of the reason for our finding is likely due to the heterogeneity of Chelyabinsk, containing both high-shock melt and low-shock clasts that record events differently. Generally, an impact with enough energy to reset the Sm-Nd chronometers would likely reset many other chronometers as well. However, it is not well understood how energetic impacts that could completely degas argon might affect more refractory dating systems. Experimental studies of shock and heat effects on Rb-Sr, Sm-Nd, Pb-Pb, and U-Pb isochrons (Gaffney et al. 2011) have been performed on a lunar basalt (described as ~60% clinopyroxene and ~30% plagioclase). A control, shocked, and

heated isochron were measured for each isotope system to monitor the effects of a ~50 GPa shock and heating of 1000 °C. The Sm-Nd system was disturbed the least, followed by Rb-Sr, with Pb-Pb and U-Pb being the most susceptible to disturbances. The authors note that shock or heating can degrade or destroy an isochron fit, but if a linear isochron remains, the age it determines likely reflects the crystallization age of the sample (based on experiments on their control sample). This provides a guide when considering Sm-Nd, Rb-Sr, and U-Pb ages, but likely does not reflect these metamorphic effects on Chelyabinsk in detail. What are the effects on the isochrons of different material that appears to have been heated to different temperatures and impacted multiple times? Chelyabinsk is thought to have experienced a shock of ~30-40 GPa and temperatures of up to ~1600 °C (Righter et al. 2015), which are different parameters than covered in the experiment. As briefly discussed before, the relative Sm-Nd, Pb-Pb, Ar-Ar age discrepancies may also represent different areas of the Chelyabinsk parent body that recorded different thermal histories before joining and being ejected with Chelyabinsk.

Righter et al. (2015) includes a compilation of measurements using different chronometers and implies that Chelyabinsk has experienced multiple impacts and has a complicated history. If each of these ages represent an impact event (at least eight suggested by Righter et al. 2015), then Chelyabinsk is indeed a heavily impacted and complex sample. However, not all of these age signatures may represent a meaningful event, or at least individual events. For example, the K-Ar ages are essentially an average of different events recorded in different minerals of the sample.

Considering the different isotopic dating methods and their context described above, a more reliable distribution of impact ages recorded by Chelyabinsk is given in Figure 5. There is strong evidence that Chelyabinsk formed at ~4560 Ma (Re-Os, Rb-Sr), and experienced an early energetic impact at ~4450 Ma (Pb-Pb, U-Pb, Sm-Nd), an impact not seen in other LL chondrites at ~2550 Ma (Ar-Ar, Sm-Nd), an impact at ~1700 Ma (Ar-Ar, Rb-Sr), and a recent impact event at ~25 Ma (Ar-Ar, Rb-Sr, U-He, U-Pb, Sm-Nd). There is also some evidence of additional impacts at ~3700 Ma (Sm-Nd) and at ~1000 Ma (Ar-Ar, Rb-Sr). Please find the references and summary of Chelyabinsk's impact history in Table 6. A less conservative approach (including the U-Pb of zircon and some of the poorly constrained ages from Rb-Sr and Sm-Nd systems) provides weak evidence of an impact event ~800 Ma.

These results provide additional data that is important for understanding the history of Chelyabinsk and the evolution of the LL chondrites. CRE ages are not typically an absolute chronometer, but the time that Chelyabinsk was closed from galactic cosmic-ray exposure is known, so in this case it is an absolute chronometer, i.e., it was ejected from its parent body ~1.2 million years ago (Righter et al. 2015). The youngest Ar-Ar age from this study places an upper limit of the most recent impact at < 30 Ma, which could be the result of an impact that is at ~1.2 Ma, though we believe these are separate events. Chelyabinsk has matching exposure ages to, and may include a shared past with, Appley Bridge (Haymann et al. 1967) and the Hayabusa target asteroid 25143 Itokawa, identified as an LL chondrite parent body (Nakamura et al. 2011, Meier et al. 2014).

Furthermore, Jourdan et al. (2017) recently completed two Ar-Ar measurements of Itokawa; one from an un-shocked grain that appeared to have an 'old' age (larger errors), and the other from a highly shocked plagioclase grain that yielded an age of 2291 ± 139 Ma. Interestingly, this age is similar (close to, but not within error) to the Ar-Ar age in

Chelyabinsk MB020f,5 (2544 ± 68 Ma) determined in this work. Although the Itokawa age is lower, the spectrum is disturbed, and >50% of the released argon is from a single step, these ages are similar to each other and not to other LL chondrites dated so far. Itokawa has a similar low-inclination orbit as Chelyabinsk, although the aphelion of Itokawa is between Mars and Earth while the aphelion for Chelyabinsk is in the asteroid belt (Popova et al. 2013).

Table 6. Impact event history of Chelyabinsk.

Event	Approximate Age (Ma)	Isotopes	Note
Formation	4560	Sr-Sr, Re-Os	LL Parent Body
Post-Accretionary Impact	4450	Pb-Pb, U-Pb, Sm-Nd	~100 Ma after formation
Impact	3700	Sm-Nd	~750 Ma later, consistent with max relict age found in Ar-Ar
Impact	2550	Ar-Ar, Sm-Nd, U-Pb	~1050 Ma later
Impact	1700	Ar-Ar, Rb-Sr	~850 Ma later
Impact	1000	Ar-Ar, Rb-Sr	~700 Ma later
Impact	25	Ar-Ar, Rb-Sr, Sm-Nd, U-Pb, U-He	~1000 Ma later, overlaps with LL CRE peak, Eugster et al. 2006
Separation from Parent	1.2	He, Ne, Ar	Righter et al. 2015

Bold events indicate high confidence, bold ages indicate contributions from this work, bold isotopes indicate high confidence. See references in Table 5.

CONCLUSIONS

Measurements from this work include Ar-Ar and U-Pb analysis of different lithologies from Chelyabinsk. We find evidence of two impact events recorded in the Ar-Ar system, and a third indicated by U-Pb.

A young impact event at **25 ± 11 Ma** significantly reset the argon in the clast-rich material, while only partially resetting the melt-rich material and leaving the high retentive phases undisturbed. Although multiple systems (Ar-Ar, U-He, U-Pb, Sm-Nd, and Rb-Sr) provide evidence for a recent event, our data provide the most precise age, and agree, within uncertainties, with the others.

The older Ar-Ar age that represents an impact energetic enough to degas and completely reset argon occurred **2544 ± 68 Ma** ago. This provides a lower limit for the time of shock alteration of minerals, including formation of high-pressure phases of argon-retentive-plagioclase (jadeite), metal and sulphide melt veins along grain boundaries, melt-filling of shock-altered silicates pore space (shock-darkening), and melt pockets. The Ar-Ar age of Itokawa has a similar age to the melt-rich material of Chelyabinsk. This may indicate a shared impact on the LL parent body that was experienced by both Chelyabinsk and Itokawa that is unique among LL chondrite ages.

The U-Pb data of apatite acquired in this study from the chondritic-textured lithology treated in concert with in-situ U-Pb data from Popova et al. (2013) yield upper and lower concordia intercepts of 4456 ± 23 and 184 ± 200 Ma, respectively. The lower intercept age resulting from a significant Pb-loss event in the apatite is likely reflected by the 25 ± 11 Ma age observed in the Ar-Ar data.

This work reports the youngest and oldest Ar-Ar ages of Chelyabinsk that are consistent with U-Pb results (this work) and with the results of other isotopic ages (e.g., Ar-Ar, Rb-Sr, Sm-Nd, U-He, U-Pb from other works). This data provides additional constraints on possible impact ages determined by other isotopic systems that might otherwise remain ambiguous. Chelyabinsk has a heavily impacted and complex history. When combined with literature data, we find strong evidence that Chelyabinsk experienced four energetic impacts after formation (~4450, ~2550, ~1700, ~25 Ma) and before cosmic-ray exposure (~1.2 Ma), with weaker evidence of additional impacts.

Acknowledgments: We would like to thank Dr. Vera Assis Fernandes for helpful and insightful discussions as well as for all her support. This work was funded by NASA Solar System Exploration Research Virtual Institute (Grant number 80NSSC20M0016 NNA14AB07A) and by The Science and Technology Development Fund, Macau SAR (File number 0105/2020/A3).

References

Badyukov D. D., Raitala J., Kostama P., and Ignatiev A. V. 2015. Chelyabinsk meteorite: Shock metamorphism, black veins and impact melt dikes, and the Hugoniot. *Petrology* 23:103–115.

Bischoff, A., Horstmann, M., Vollmer, C., Heitmann, U., and Decker, S. 2013. Chelyabinsk—not only another ordinary LL5 chondrite, but a spectacular chondrite breccia (abstract). *Meteoritics and Planetary Science Supplement*, 76, p.5171.

Brown, P.G., Assink, J.D., Astiz, L., Blaauw, R., Boslough, M.B., Borovic̆ka, J., Brachet, N., Brown, D., Campbell-Brown, M., Ceranna, L., Cooke, W., de Groot-Hedlin, C., Drob, D.P., Edwards, W., Evers, L.G., Garces, M., Gill, J., Hedlin, M., Kingery, A., Laske, G., Le Pichon, A., Mialle, P., Moser, D.E., Saffer, A., Silber, E., Smets, P., Spalding, R.E., Spurný, P., Tagliaferri, E., Uren, D., Weryk, R.J., Whitaker, R., and Krzeminski, Z. 2013. A 500-kiloton airburst over Chelyabinsk and an enhanced hazard from small impactors. *Nature* 503:238–241.

Bogard, D. D. 1995. Impact ages of meteorites: A synthesis. *Meteoritics* 30:244-268.

Bogomolova E. S., Skublov S. G., Marin Y. B, Stepanov S. Y., Antonov A. V., and Galankina O. L. 2013. Sm–Nd age and isotope geochemistry of minerals of the Chelyabinsk meteorite. *Doklady Earth Sciences* 452:1034–1038.

Bouvier A. 2013. Pb-Pb chronometry of the dark melt lithology of the Chelyabinsk LL chondrite. *Large Meteorite Impacts and Planetary Evolution V*:1737,3087.

Cherniak D. J., Lanford W. A., and Ryerson F. J. 1991. Lead diffusion in apatite and zircon using ion implantation and Rutherford backscattering techniques. *Geochimica et Cosmochimica Acta* 55:1663-1673.

Chew D.M., Sylvester P.J., and Tubrett M.N. 2011. U-Pb and Th-Pb Dating of Apatite by LA-ICP-MS. *Chemical Geology* 280:200-216.

Day J. M. D., Corder C. A., Dhaliwal J. K., Liu Y., and Taylor L. A. 2014. The Chelyabinsk fall highly siderophile element abundance and $^{187}\text{Os}/^{188}\text{Os}$ composition and comparison with ordinary and carbonaceous chondrites (abstract #5078). *77th Annual Meeting of the Meteoritical Society* 77:5078.

Deino, A. L. 2001. Users manual for Mass Spec v. 5.02. Berkeley Geochronology Center Special Publication 1a:119.

Eugster, O., Herzog, G. F., Marti, K., & Caffee, M. W. (2006). Irradiation records, cosmic-ray exposure ages, and transfer times of meteorites. *Meteorites and the early solar system II*, (943), 829-851. Gaffney A. M., Borg L. E., Asmerom Y., Shearer C. K., and

- Burger P. V. 2011. Disturbance of isotope systematics during experimental shock and thermal metamorphism of a lunar basalt with implications for Martian meteorite chronology. *Meteoritics & Planetary Science* 46:35–52.
- Galimov, E. M. 2013. Chelyabinsk meteorite - an LL5 chondrite. *Solar System Research* 47:255-259.
- Haba M. K., Sumino H., Nagao K., Mikouchi T., Komatsu M., and Zolensky M. E. 2014. Noble gases in the Chelyabinsk meteorite (abstract #1732). 45th Lunar and Planetary Science Conference.
- Heymann D., Anders E., and Rowe M. W. 1967, Meteorites with short cosmic-ray exposure ages. *Geochimica et Cosmochimica Acta* 31:1791-1809.
- Jourdan F., Andreoli M.A.G., McDonald I., and Maier W.D. 2010. $^{40}\text{Ar}/^{39}\text{Ar}$ thermochronology of the fossil LL6-chondrite from the Morokweng crater. South Africa, *Geochimica et Cosmochimica Acta* 74:1734–1747.
- Jourdan F., Timms N. E., Eroglu E., Mayers C., Frew A., Bland P. A., Collins G. S., Davison T. M., Abe M., and Yada T. 2017. Collisional history of asteroid Itokawa. *Geology* 45:819–822.
- Kamioka M., Terada K., Hidaka H., Kimura K., and Skublov S. 2014. Secondary ion mass spectrometry (SHRIMP) U-Pb dating of Chelyabinsk meteorite. The 62nd Annual Conference on Mass Spectrometry 62:2.
- Lapen T. J., Kring D. A., Zolensky M. E., Andreasen R., Righter M., Swindle T. D., and Beard S. P. 2014. Uranium-lead isotope evidence in the Chelyabinsk LL5 chondrite meteorite for ancient and recent thermal events (abstract #2561). 45th Lunar and Planetary Science Conference.
- Lindsay F. N., Herzog G. F., Park J., Turrin B. D., Delaney J. S., and Swisher C. C. 2015. Chelyabinsk Ar ages—A young heterogeneous LL5 chondrite (abstract). Lunar and Planetary Science Conference 46:2226.
- McConville P., Kelley S. and Turner G. 1988). Laser probe ^{40}Ar - ^{39}Ar studies of the Peace River shocked L6 chondrite. *Geochimica et Cosmochimica Acta* 52:2487–2499.
- Meier M. M. M., Alwmark C., Bajt S., Böttger U., Busemann H., Fujiya W., Gilmour J., Heitmann U., Hoppe P., Hübers H.-W., Marone F., Ott U., Pavlov S., Schade U., Spring N., Stampanoni M., and Weber I. 2014. A precise cosmic-ray exposure age for an olivine grain from the surface of near-Earth asteroid (25143) Itokawa (abstract #1247). 45th Lunar and Planetary Science Conference.
- Min K., Reiners P. W., and Shuster D. L. 2013. (U-Th)/He ages of phosphates from St. Séverin LL6 chondrite. *Geochimica et Cosmochimica Acta* 100:282–296.

Nakamura T., Noguchi T., Tanaka M., Zolensky M. E., Kimura M., Tsuchiyama A., Nakato A., Ogami T., Ishida H., Uesugi M., Yada T., Shirai K., Fujimura A., Okazaki R., Sandford S. A., Ishibashi Y., Abe M., Okada T., Ueno M., Mukai T., Yoshikawa M., and Kawaguchi J. 2011. Itokawa dust particles: A direct link between S-type asteroids and ordinary chondrites. *Science* 333:1113–1116.

Petrova E. V., Grokhovsky V. I., and Muftakhetdinova R. F. 2016. Heat treatment of the different structure zones in the Chelyabinsk meteorite (abstract #6487). *Meteoritics & Planetary Science* 51:513.

Popova, O. P., Jenniskens, P., Emel'yanenko, V., Kartashova, A., Biryukov, E., Khaibrakhmanov, S., and Mikouchi, T. 2013. Chelyabinsk airburst, damage assessment, meteorite recovery, and characterization. *Science* 342:1069-1073.

Reed, B.C. 1989. Linear least-squares fits with errors in both coordinates. *American Journal of Physics* 57:642-647.

Renne P. R., Balco G., Ludwig K. R., Mundil R., and Min K. 2011. Response to the comment by W. H. Schwarz et al. on “Joint determination of ^{40}K decay constants and $^{40}\text{Ar}^*/^{40}\text{K}$ for the Fish Canyon sanidine standard, and improved accuracy for $^{40}\text{Ar}/^{39}\text{Ar}$ geochronology” by P. R. Renne et al. (2010). *Geochimica et Cosmochimica Acta* 75:5097–5100.

Righter K., Abell P., Agresti D., Berger E. L., Burton A. S., Delaney J. S., Fries M. D., Gibson E. K., Haba M. K., Harrington R., Herzog G. F., Keller L. P., Locke D., Lindsay F. N., McCoy T. J., Morris R. V., Nagao K., Nakamura-Messenger K., Niles P. B., Nyquist L. E., Park J., Peng Z. X., Shih C.-Y., Simon J. I., Swisher C. C. III, Tappa M. J., Turrin B. D., and Zeigler R. A. 2015. Mineralogy, petrology, chronology, and exposure history of the Chelyabinsk meteorite and parent body. *Meteoritics & Planetary Science* 50:1790–1819.

Sarafian AR, Hauri EH, McCubbin FM, Lapen TJ, Berger EL, Nielsen SG, Marschall HR, Gaetani GA, Righter K, and Sarafian E. 2017. Early accretion of water and volatile elements to the inner Solar System: evidence from angrites. *Philosophical Transactions of the Royal Society A: Mathematical, Physical and Engineering Sciences* 375:1-27.

Shaulis B., Lapen T. J., and Toms A. 2010. Signal linearity of an extended range pulse counting detector: Applications to accurate and precise U-Pb dating of zircon by laser ablation quadrupole ICP-MS. *Geochemistry, Geophysics, Geosystems* 11:11.

Skublov S. G., Guseva N. S., Presnyakov S. L., Li X.-H., Marin Yu. B., Sergeev S. A., Berezhnaya N. G., Tyuleneva N. V., and Alekseev V. I. 2015. U-Pb age of zircon and the

history of impact transformations of the Chelyabinsk meteorite. *Doklady Earth Sciences* 462:586–591.

Swindle, T. D., Kring, D. A., Olson, E. K., and Isachsen, C. E. 2006. Ar-Ar Dating of Shock-melted Ordinary Chondrites: Chronology of Asteroidal Impacts 37th Annual Lunar and Planetary Science Conference.

Swindle, T. D., Isachsen, C. E., Weirich, J. R., and Kimura, M. 2011. ^{40}Ar - ^{39}Ar studies of shocked L6 chondrites Allan Hills 78003, Yamato 74445, and Yamato 791384 (abstract). Lunar and Planetary Science Conference 42:1897.

Swindle, T. D., Kring, D. A., and Weirich, J. R. 2014. ^{40}Ar - ^{39}Ar ages of impacts involving ordinary chondrite meteorites. In F. Jourdan, D. Mark, and C. Verati (Eds.), $^{40}\text{Ar}/^{39}\text{Ar}$ dating: from geochronology to thermochronology, from archaeology to planetary sciences. London: Geological Society 378:334-347

Swindle, T. D. and Weirich, J.R. 2017. The effect of partial thermal resetting on ^{40}Ar - ^{39}Ar “Plateaus” (abstract). Lunar and Planetary Science Conference 48:1265.

Takagami, Y. and I. Kaneoka. 1987. Investigations of the effect of shock on the Antarctic meteorites by the ^{40}Ar - ^{39}Ar method. *Proceedings of the NIPR Symposium on Antarctic Meteorites* 11:133-143.

Thomson, S.N., Gehrels, G.E., Ruiz, J., and Buchwaldt, R. 2012. Routine low-damage apatite U–Pb dating using laser ablation-multicollector-ICPMS. *Geochemistry, Geophysics, Geosystems* 13:2.

Trieloff M., Korochantseva, E. V., A. I. Buikin, J. Hopp, M. A. Ivanova, and A. V. Korochantsev. 2018. The Chelyabinsk meteorite: Thermal history and variable shock effects recorded by the ^{40}Ar - ^{39}Ar system. *Meteoritics & Planetary Science* 53:343-358.

Walton, C.R., Shorttle, O., Hu, S., Rae, A.S., Jianglong, J., Černok, A., Williams, H., Liu, Y., Tang, G., Li, Q. and Anand, M. 2022. Ancient and recent collisions revealed by phosphate minerals in the Chelyabinsk meteorite. *Communications Earth & Environment* 3:1-9.

Weirich J. R., Isachsen C., Swindle T. D., and Kring D. A. 2009. Ar-Ar impact ages of shocked LL chondrites (abstract #5368). *Meteoritics & Planetary Science* 44:215.

Supplementary Materials

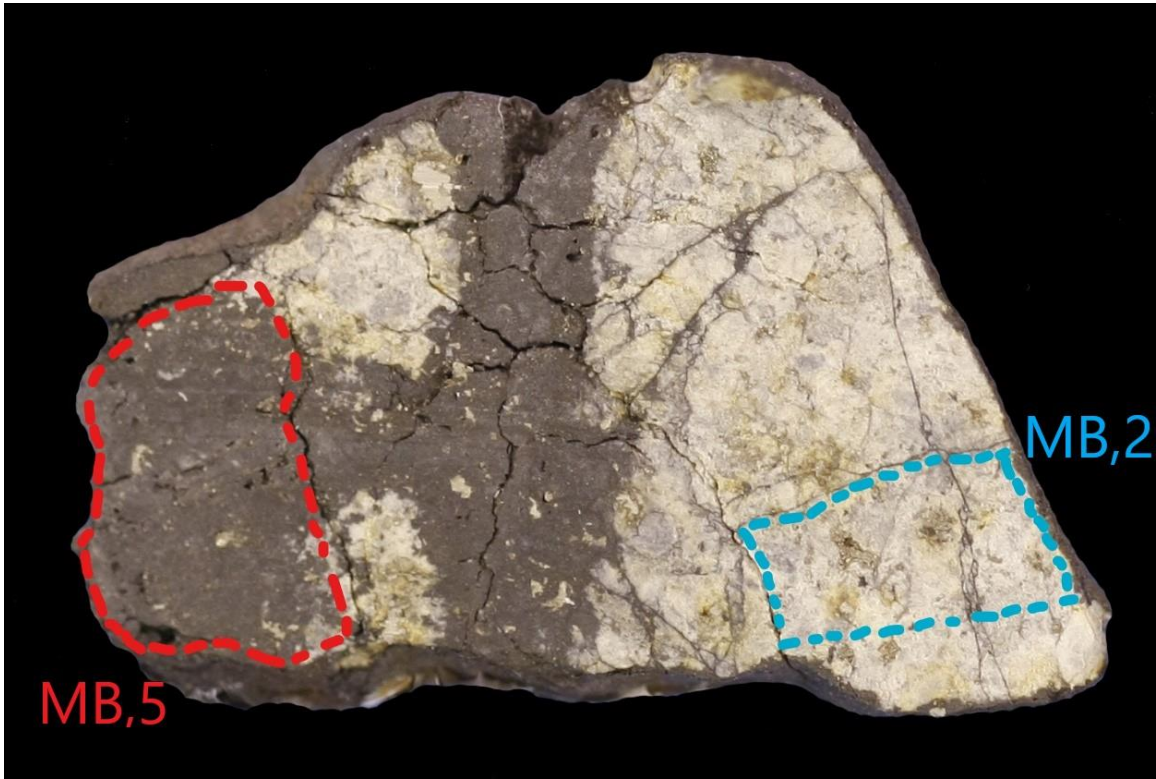


Figure S1. Image of Chelyabinsk sample (width = 1.98 cm) that shows regions used for Ar-Ar measurements; MB,2 is the light lithology and MB,5 is the dark melt-rich lithology (see respective Ar results in Figs. 2 and 3).

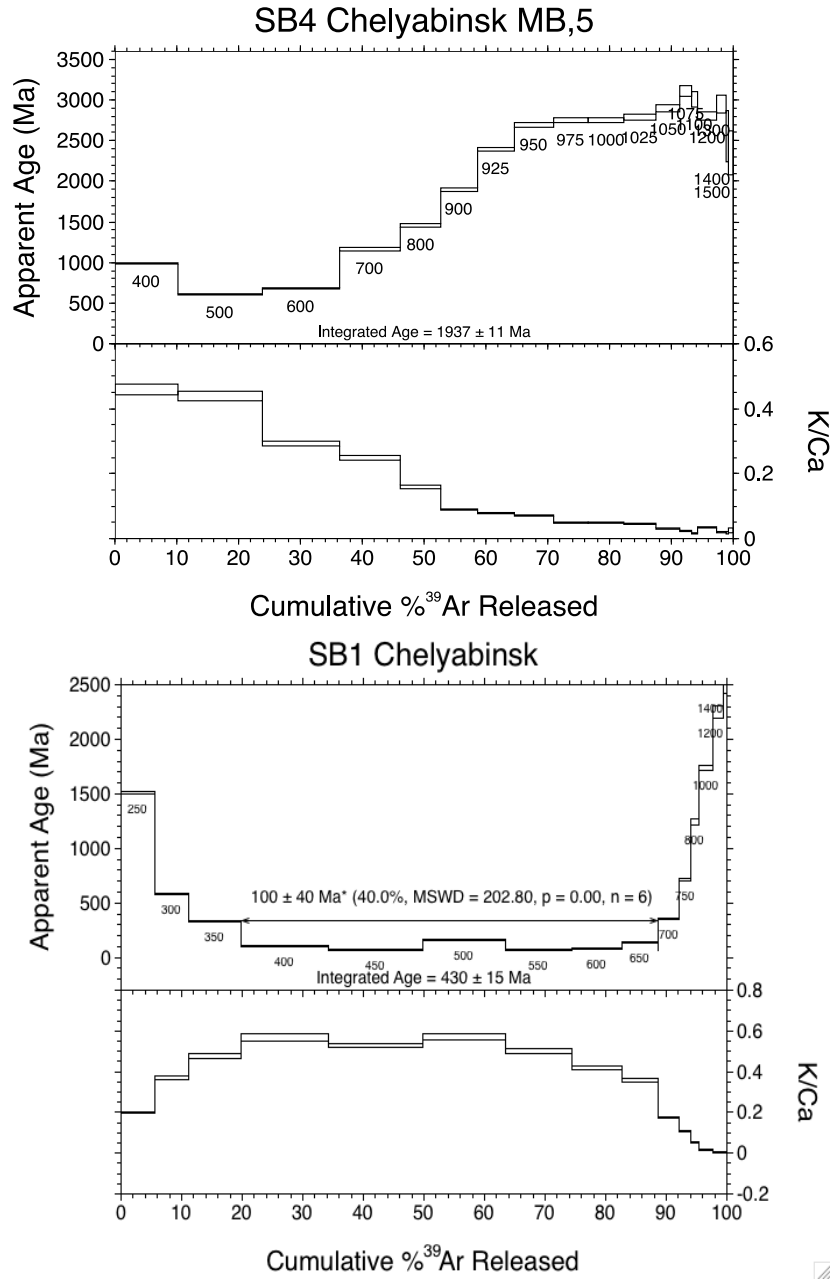


Figure S2. Argon age spectra (no trapped corrections) of split SB4 (top) from MB020f,5 and split SB1 from MB020f,2 (bottom) with the K/Ca release, which is similar to Chelyabinsk analysis shown in Trieloff et al., 2018.

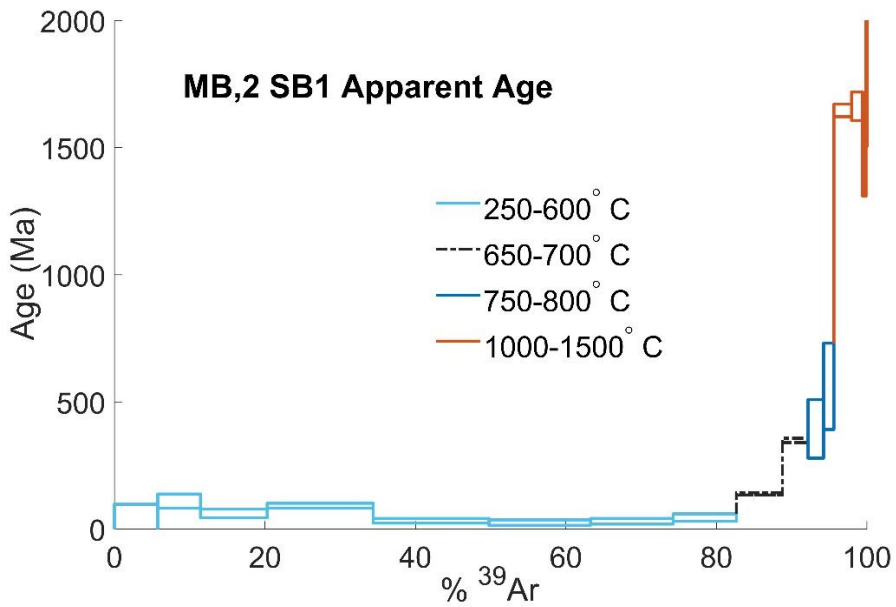
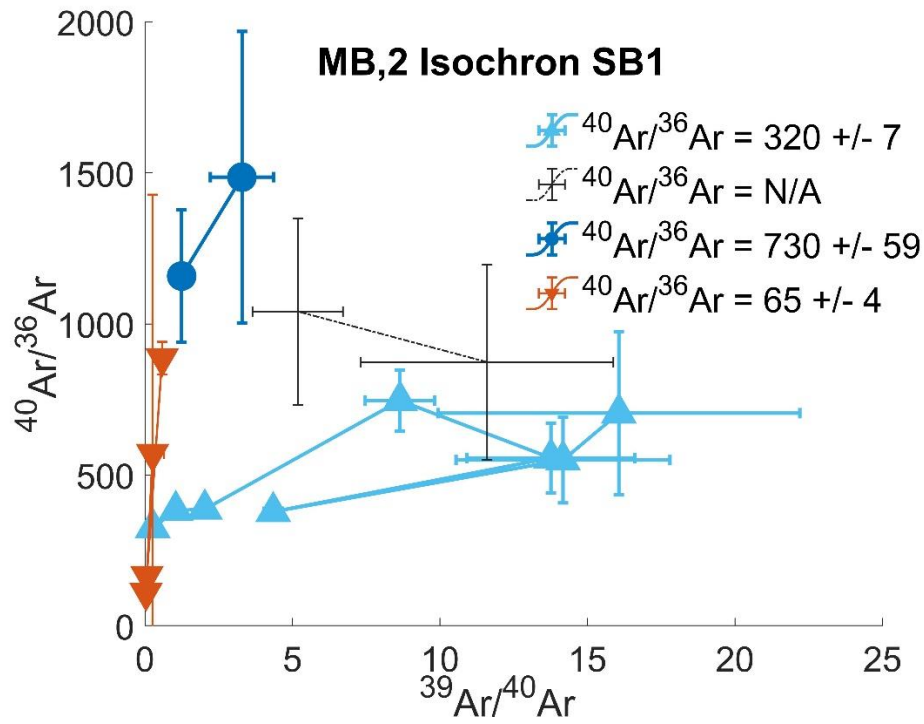


Figure S3. Isochron plot (top) and apparent age spectra (bottom) for split SB1 of MB,2. Isochron data shows multiple trapped components which was used to make appropriate corrections to the corresponding (matching colors) temperature steps.

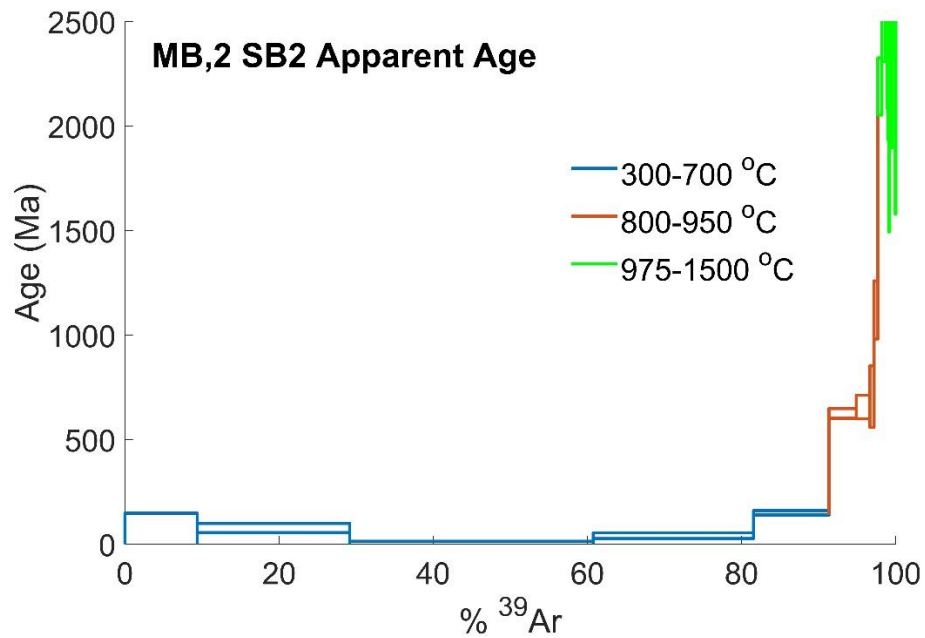
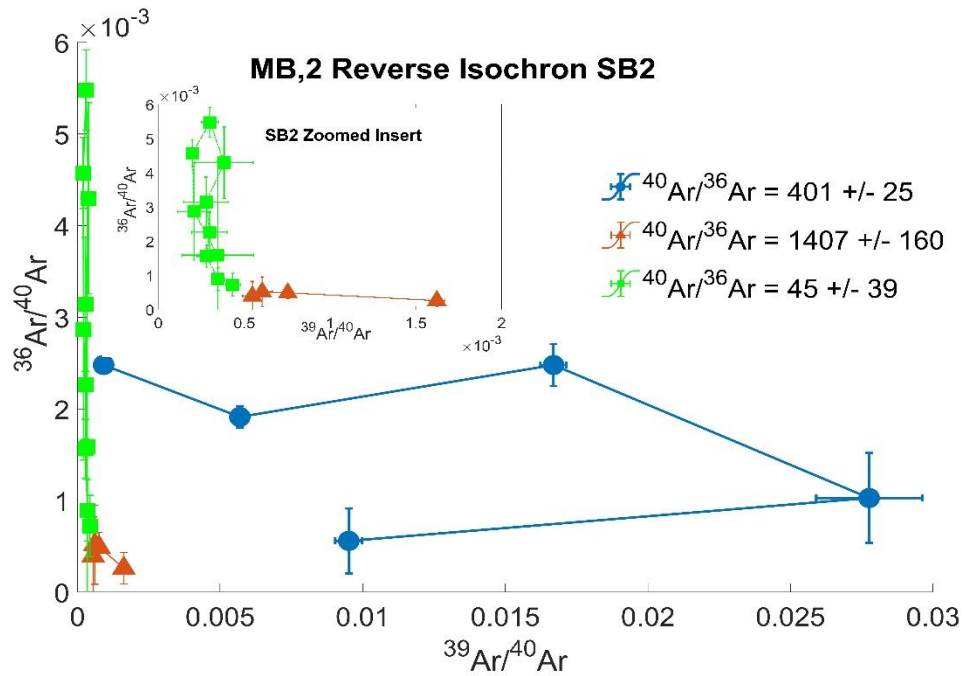


Figure S4. Reverse isochron plot (top) and apparent age spectra (bottom) for split SB2 of MB,2. Isochron data shows multiple trapped components which was used to make appropriate corrections to the corresponding (matching colors) temperature steps. Inclusion/exclusion of the 700°C step doesn't significantly affect results.

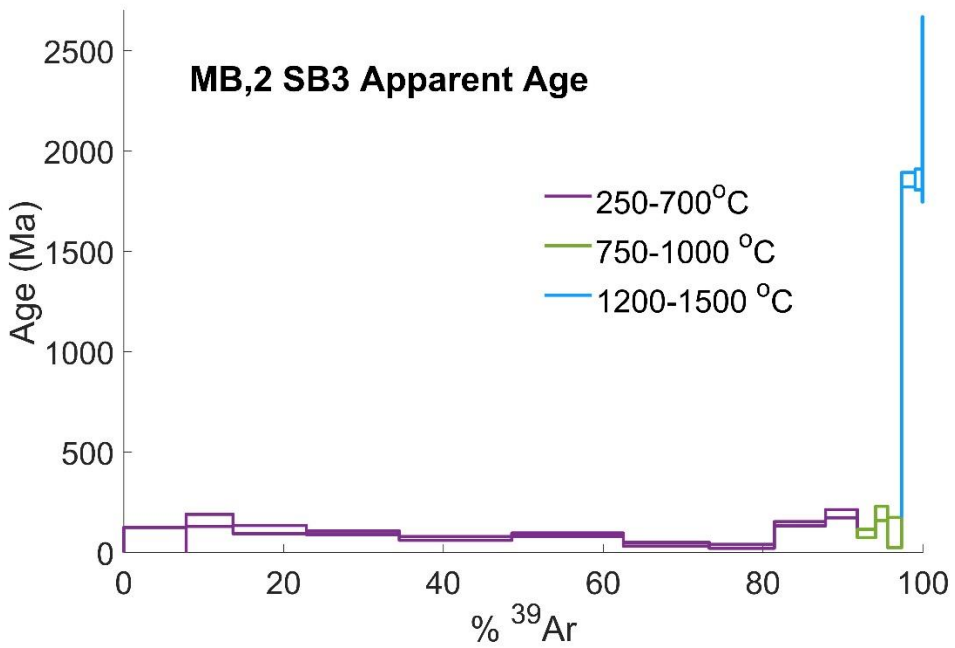
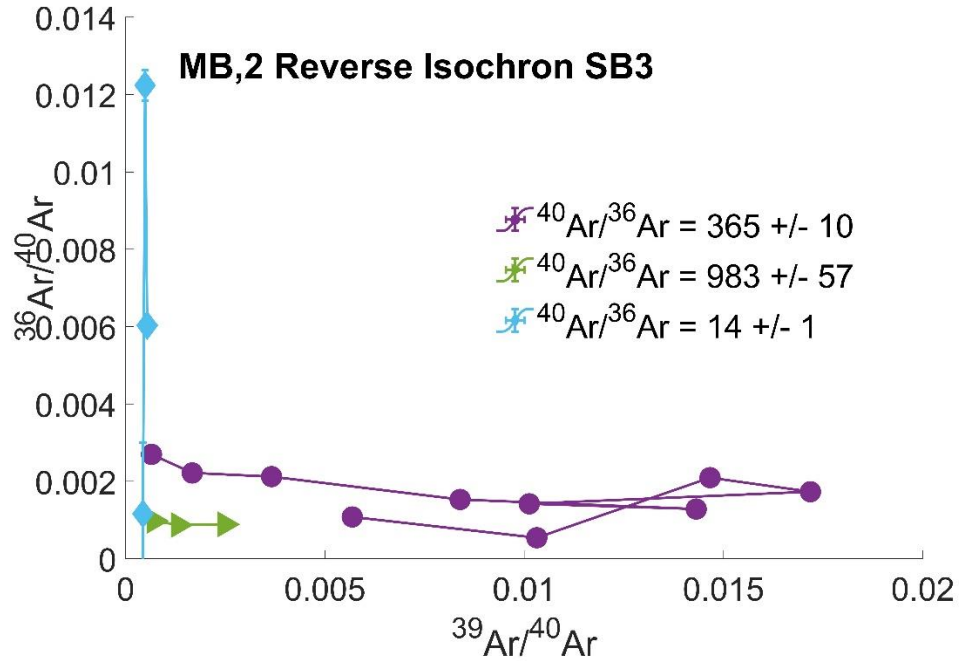


Figure S5. Reverse isochron plot (top) and apparent age spectra (bottom) for split SB3 of MB,2. Isochron data shows multiple trapped components which was used to make appropriate corrections to the corresponding (matching colors) temperature steps. Inclusion/exclusion of the 700°C step doesn't significantly affect results.

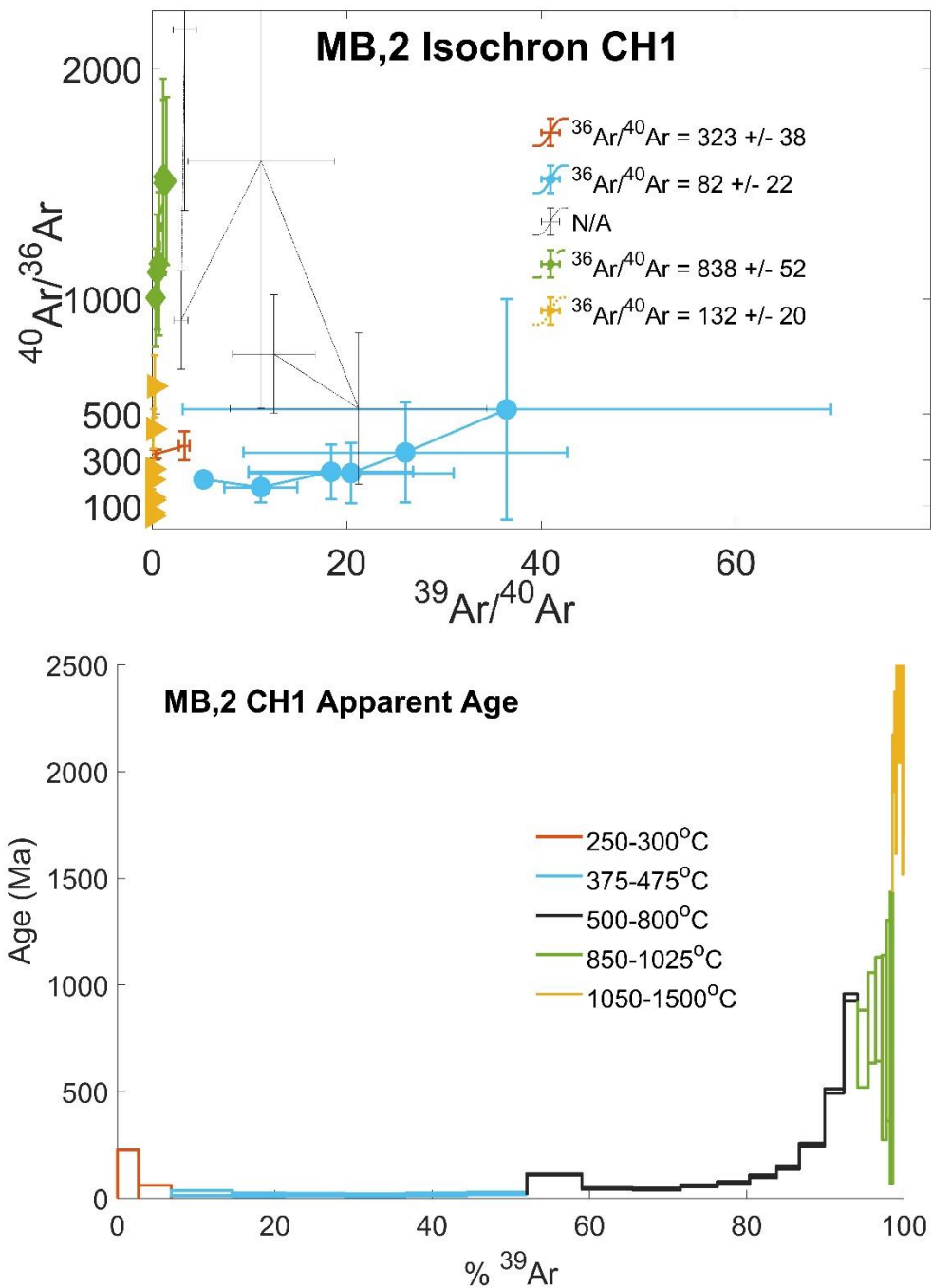


Figure S6. Isochron plot (top) and apparent age spectra (bottom) for split CH1 of MB,2. Isochron data shows multiple trapped components which was used to make appropriate corrections to the corresponding (matching colors) temperature steps. Isochron values from temperature steps 550-650°C have very large errors and were removed from the isochron plot to obtain best results.

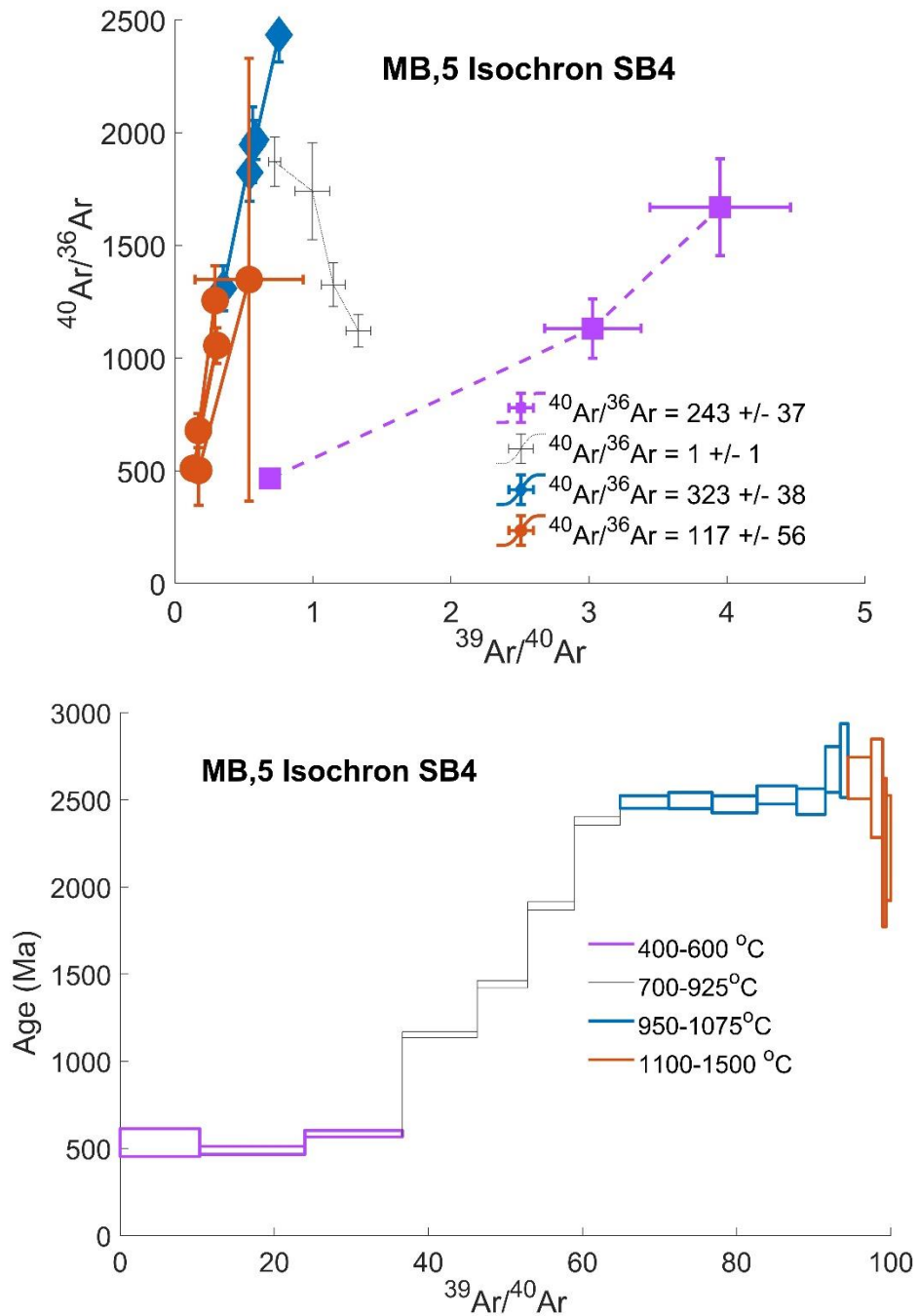


Figure S7. Isochron plot (top) and apparent age spectra (bottom) for split SB4 of MB.5. Isochron data shows multiple trapped components which was used to make appropriate corrections to the corresponding (matching colors) temperature steps.

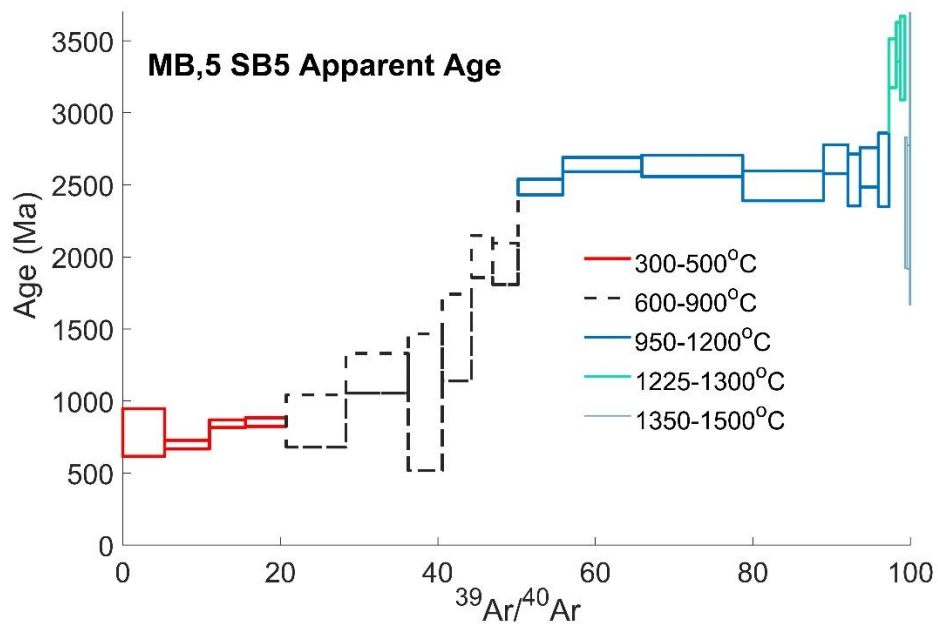
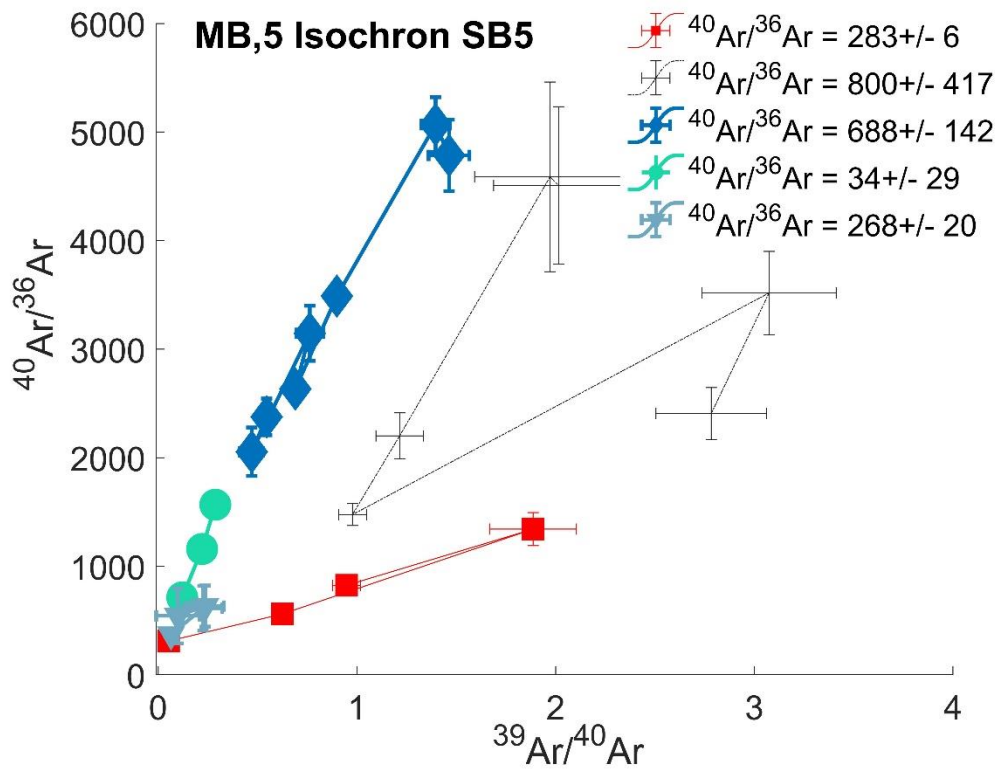


Figure S8. Isochron plot (top) and apparent age spectra (bottom) for split SB5 of MB,5. Isochron data shows multiple trapped components which was used to make appropriate corrections to the corresponding (matching colors) temperature steps.

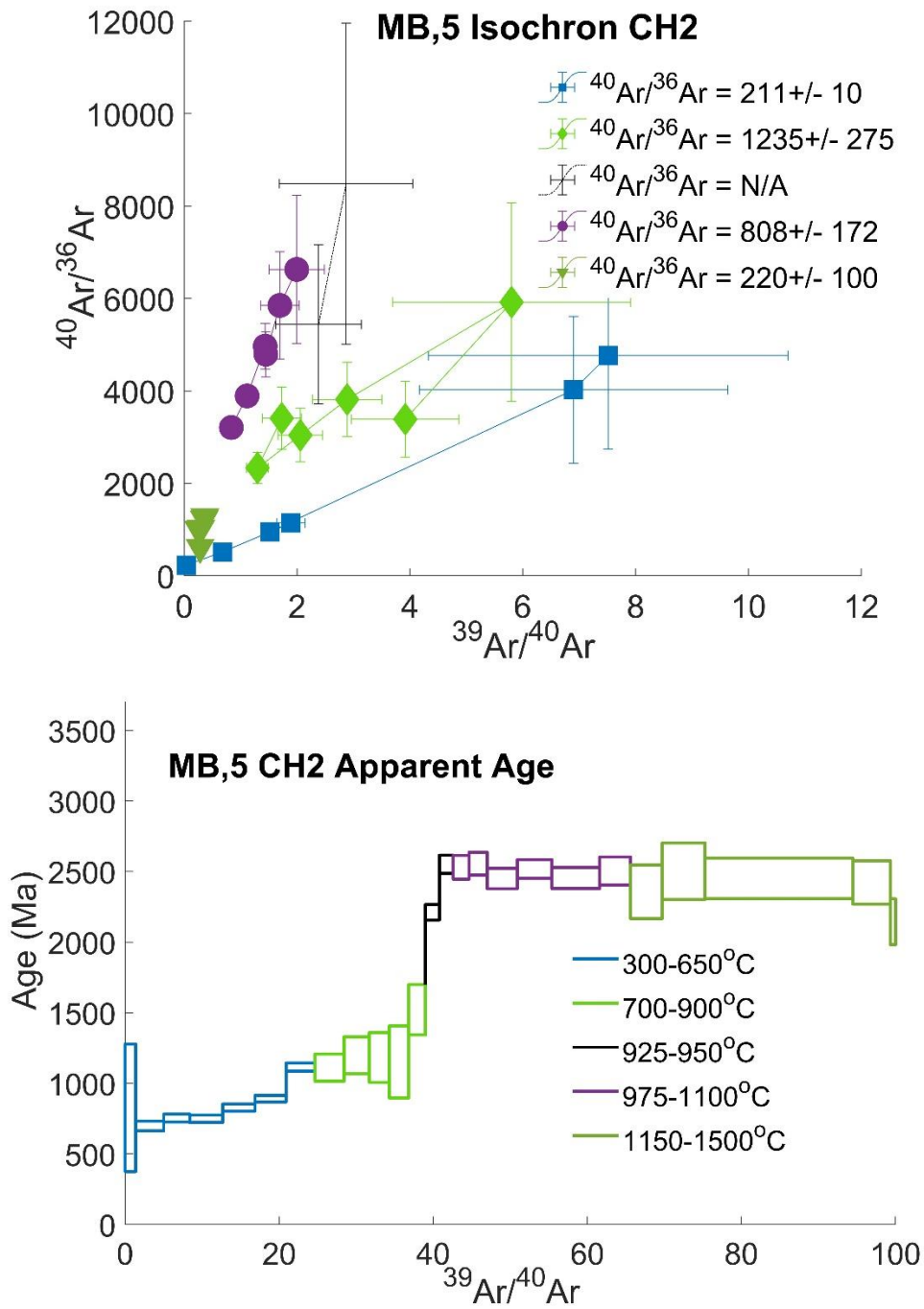


Figure S9. Isochron plot (top) and apparent age spectra (bottom) for split SB4 of MB,5. Isochron data shows multiple trapped components which was used to make appropriate corrections to the corresponding (matching colors) temperature steps.

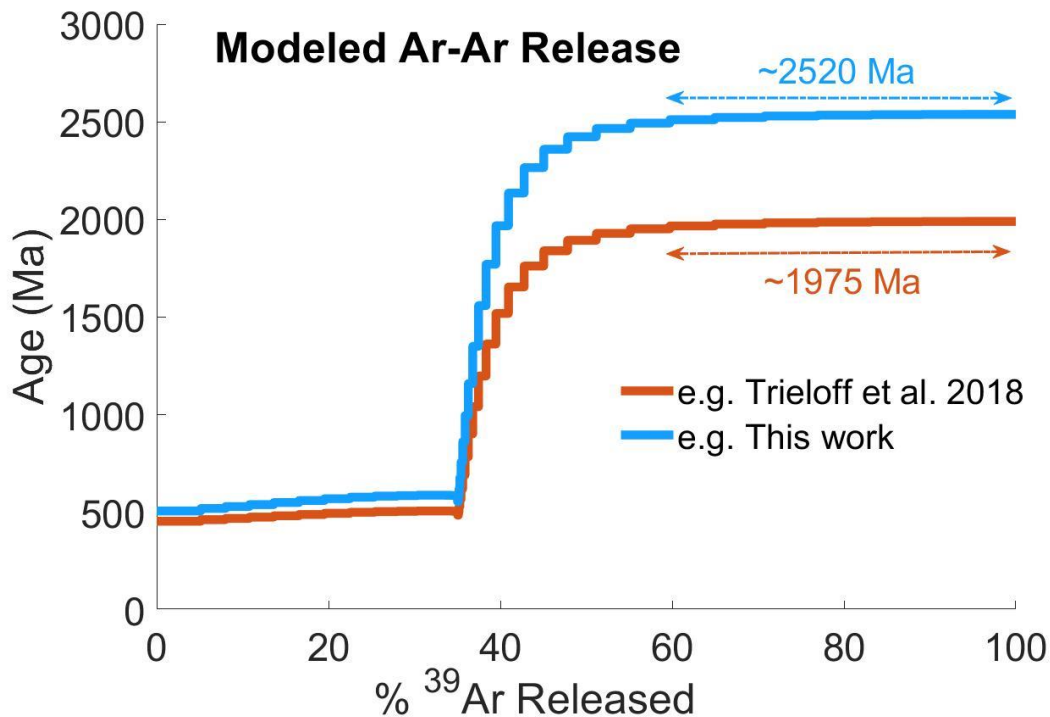


Figure S10. Model (Swindle and Weirich 2017), of partial resetting of an event sample of Chelyabinsk (similar to CH2 in this work) that demonstrates partial resetting of a sample that was completely degassed/reset at 2550 Ma. The age from 60-100% of the released argon is 2520 Ma. The model assumes that argon was released from two mineral phases (first 35% of gas released under $E = 15$ kcal/mol conditions, with the remaining 65% released under $E = 70$ kcal/mol), with a heating pulse that reached 1100 °C for 120 seconds. Note that the results are not unique; various combinations of E values and heat pulse can achieve the same result. The same model was used to show the result of partial resetting of a sample that was completely degassed at 2000 Ma (similar to results from Trieloff et al. 2018) under similar conditions. The age from 60-100% of the released argon is 1975 Ma. Preliminary conclusions are that these results represent unique impacts. Further emphasis on model parameters and results will be the topic of future work.

Sample	Mass (mg)	J Factor	Split							
MB020f,2	10.3	1.06E-03	CH1							
Step #	Temp (°C)	⁴⁰ Ar	³⁹ Ar	³⁸ Ar	³⁷ Ar	³⁶ Ar	Apparent Age	± 2σ		
1	250	797.0 ± 11.5	0.930 ± 0.025	0.615 ± 0.028	3.336 ± 0.365	2.536 ± 0.116	18.507	208.732		
2	300	154.8 ± 5.3	1.417 ± 0.018	0.191 ± 0.022	2.732 ± 0.347	0.489 ± 0.062	22.442	38.656		
3	350	109.1 ± 5.1	2.661 ± 0.013	0.142 ± 0.022	3.195 ± 0.332	0.515 ± 0.062	24.873	12.174		
4	375	37.6 ± 4.6	2.312 ± 0.022	0.087 ± 0.022	2.917 ± 0.325	0.221 ± 0.059	16.960	6.990		
5	400	35.1 ± 4.5	2.593 ± 0.016	0.050 ± 0.022	2.681 ± 0.324	0.142 ± 0.058	17.180	5.540		
6	425	31.5 ± 4.5	2.651 ± 0.015	0.094 ± 0.020	2.914 ± 0.323	0.155 ± 0.057	14.954	5.415		
7	450	34.2 ± 4.4	2.670 ± 0.025	0.096 ± 0.021	2.819 ± 0.318	0.132 ± 0.056	18.272	5.155		
8	475	37.1 ± 4.4	2.599 ± 0.026	0.091 ± 0.020	2.673 ± 0.319	0.102 ± 0.056	22.727	5.126		
9	500	146.3 ± 4.4	2.410 ± 0.020	0.128 ± 0.022	2.786 ± 0.329	0.234 ± 0.055	111.915	3.428		
10	525	54.6 ± 4.3	2.215 ± 0.025	0.091 ± 0.021	2.646 ± 0.323	0.134 ± 0.055	46.223	3.676		
11	550	47.8 ± 4.3	2.077 ± 0.022	0.068 ± 0.020	2.252 ± 0.312	0.058 ± 0.055	43.263	3.895		
12	575	50.0 ± 4.3	1.598 ± 0.013	0.059 ± 0.020	2.073 ± 0.312	0.028 ± 0.054	58.582	4.989		
13	600	55.3 ± 4.3	1.421 ± 0.010	0.028 ± 0.020	1.895 ± 0.309	0.022 ± 0.054	72.610	5.558		
14	625	65.6 ± 4.3	1.169 ± 0.013	0.046 ± 0.020	1.698 ± 0.307	0.081 ± 0.055	103.767	6.715		
15	650	79.1 ± 4.3	0.997 ± 0.007	0.062 ± 0.019	1.551 ± 0.308	0.046 ± 0.054	144.958	7.657		
16	700	156.1 ± 4.3	1.096 ± 0.008	0.093 ± 0.020	2.257 ± 0.311	0.138 ± 0.056	252.538	6.895		
17	750	255.1 ± 4.4	0.839 ± 0.013	0.097 ± 0.020	3.238 ± 0.316	0.304 ± 0.056	502.629	10.415		
18	800	392.9 ± 4.6	0.607 ± 0.012	0.137 ± 0.021	3.848 ± 0.331	0.245 ± 0.056	941.219	17.602		
19	850	462.1 ± 4.7	0.460 ± 0.012	0.167 ± 0.021	5.016 ± 0.342	0.375 ± 0.063	701.436	181.692		
20	900	421.0 ± 4.6	0.333 ± 0.009	0.194 ± 0.021	6.347 ± 0.340	0.371 ± 0.057	846.066	212.522		
21	950	378.4 ± 4.6	0.290 ± 0.008	0.160 ± 0.021	8.425 ± 0.369	0.321 ± 0.059	886.651	243.505		
22	975	302.4 ± 4.6	0.187 ± 0.008	0.128 ± 0.021	8.814 ± 0.349	0.315 ± 0.060	707.660	432.567		
23	1000	355.0 ± 4.7	0.167 ± 0.007	0.171 ± 0.022	12.980 ± 0.359	0.393 ± 0.061	833.427	469.547		
24	1025	330.6 ± 4.4	0.124 ± 0.007	0.210 ± 0.025	18.615 ± 0.506	0.429 ± 0.059	753.012	682.075		
25	1050	196.6 ± 4.3	0.091 ± 0.006	0.195 ± 0.025	19.533 ± 0.215	0.410 ± 0.058	2038.819	135.455		
26	1075	150.5 ± 4.2	0.061 ± 0.006	0.215 ± 0.025	20.046 ± 0.470	0.448 ± 0.056	2163.876	210.875		
27	1100	142.5 ± 4.1	0.050 ± 0.004	0.242 ± 0.023	15.175 ± 0.314	0.640 ± 0.066	1902.807	288.454		
28	1150	947.4 ± 4.2	0.094 ± 0.006	0.979 ± 0.025	21.098 ± 0.329	4.515 ± 0.088	3175.227	381.275		
29	1200	797.2 ± 4.3	0.095 ± 0.008	1.223 ± 0.031	27.707 ± 0.438	5.890 ± 0.094	3059.342	1018.369		
30	1300	460.9 ± 16.7	0.130 ± 0.011	1.477 ± 0.020	28.452 ± 0.282	6.629 ± 0.095	1744.146	569.118		
31	1400	89.2 ± 16.2	0.056 ± 0.009	0.378 ± 0.019	3.785 ± 0.129	1.610 ± 0.087	582.308	679.414		
32	1500	59.2 ± 17.5	0.017 ± 0.012	0.108 ± 0.020	-0.579 ± 0.145	0.482 ± 0.092	2130.363	1030.545		
Total							185.6	15.9		

All isotope values are in 1e-8 ccSTP/g and ages are in Ma. This data has been blank corrected only.

Sample	Mass (mg)	J Factor	Split							
MB020f,2	10.06	1.062E-03	SB1							
Step #	Temp (°C)	⁴⁰ Ar	³⁹ Ar	³⁸ Ar	³⁷ Ar	³⁶ Ar	Apparent Age	± 2σ		
1	250	1274.3 ± 4.4	1.035 ± 0.012	0.794 ± 0.013	2.652 ± 0.037	3.952 ± 0.051	36.4	61.2		
2	300	371.3 ± 3.0	1.018 ± 0.012	0.225 ± 0.005	1.397 ± 0.027	0.992 ± 0.038	110.1	27.7		
3	350	302.7 ± 3.0	1.591 ± 0.015	0.186 ± 0.005	1.690 ± 0.035	0.797 ± 0.035	61.7	16.8		
4	400	218.3 ± 2.9	2.531 ± 0.018	0.143 ± 0.005	2.770 ± 0.101	0.331 ± 0.035	92.0	9.5		
5	450	111.3 ± 2.7	2.758 ± 0.021	0.126 ± 0.007	2.975 ± 0.073	0.237 ± 0.036	32.5	9.3		
6	500	210.3 ± 2.5	2.420 ± 0.017	0.182 ± 0.007	2.396 ± 0.063	0.588 ± 0.035	25.4	10.7		
7	550	76.4 ± 2.5	1.973 ± 0.016	0.077 ± 0.005	2.328 ± 0.067	0.157 ± 0.031	30.7	11.2		
8	600	66.0 ± 2.5	1.505 ± 0.014	0.060 ± 0.006	2.014 ± 0.057	0.110 ± 0.031	45.2	14.5		
9	650	82.9 ± 2.4	1.102 ± 0.012	0.050 ± 0.006	1.793 ± 0.053	0.108 ± 0.031	138.5	4.2		
10	700	122.2 ± 2.4	0.609 ± 0.010	0.051 ± 0.004	2.063 ± 0.073	0.132 ± 0.030	348.5	8.4		
11	750	166.9 ± 2.5	0.371 ± 0.008	0.073 ± 0.006	2.204 ± 0.067	0.143 ± 0.032	393.8	115.1		
12	800	229.3 ± 2.5	0.249 ± 0.007	0.079 ± 0.006	2.703 ± 0.067	0.224 ± 0.033	561.2	169.7		
13	1000	637.2 ± 3.0	0.432 ± 0.009	0.328 ± 0.008	17.320 ± 0.215	0.845 ± 0.038	1646.3	24.6		
14	1200	620.6 ± 2.3	0.299 ± 0.008	1.173 ± 0.020	51.385 ± 0.390	4.057 ± 0.040	1662.5	55.8		
15	1400	238.0 ± 10.4	0.089 ± 0.007	0.513 ± 0.037	12.299 ± 0.174	2.224 ± 0.119	1498.1	189.5		
16	1500	52.0 ± 11.3	0.024 ± 0.007	0.012 ± 0.040	0.190 ± 0.034	0.091 ± 0.122	2023.7	518.7		
Total							191.4	6.7		

All isotope values are in 1e-8 ccSTP/g and ages are in Ma. This data has been blank corrected only.

Sample	Mass (mg)	J Factor	Split						
MB020f,2	10.3	1.062E-03	SB2						
Step #	Temp (°C)	⁴⁰ Ar	³⁹ Ar	³⁸ Ar	³⁷ Ar	³⁶ Ar	Apparent Age	± 2σ	
1	300	1881.5 ± 10.2	1.720 ± 0.018	0.993 ± 0.014	1.773 ± 0.068	4.730 ± 0.077	12.5	135.3	
2	400	637.5 ± 9.7	3.629 ± 0.024	0.367 ± 0.007	3.615 ± 0.071	1.281 ± 0.064	76.8	22.0	
3	500	347.1 ± 9.3	5.798 ± 0.032	0.336 ± 0.010	6.929 ± 0.171	0.930 ± 0.066	12.3	14.7	
4	600	137.3 ± 9.2	3.815 ± 0.021	0.164 ± 0.006	5.291 ± 0.148	0.202 ± 0.059	40.1	14.0	
5	700	188.9 ± 9.1	1.799 ± 0.021	0.099 ± 0.005	3.086 ± 0.099	0.144 ± 0.058	149.8	10.5	
6	800	400.2 ± 9.3	0.651 ± 0.009	0.091 ± 0.005	2.413 ± 0.107	0.146 ± 0.060	624.9	23.7	
7	900	427.4 ± 9.6	0.326 ± 0.009	0.142 ± 0.005	5.605 ± 0.086	0.275 ± 0.061	655.3	56.3	
8	925	163.9 ± 9.7	0.102 ± 0.008	0.097 ± 0.007	3.823 ± 0.111	0.138 ± 0.062	705.6	147.2	
9	950	167.7 ± 9.7	0.095 ± 0.008	0.096 ± 0.006	4.787 ± 0.094	0.121 ± 0.062	1120.3	138.6	
10	975	214.8 ± 9.9	0.097 ± 0.008	0.125 ± 0.007	5.758 ± 0.199	0.218 ± 0.063	2189.4	136.8	
11	1000	223.3 ± 10.0	0.083 ± 0.008	0.165 ± 0.007	8.290 ± 0.233	0.284 ± 0.065	2468.6	159.7	
12	1025	159.3 ± 5.8	0.051 ± 0.009	0.177 ± 0.006	10.339 ± 0.226	0.336 ± 0.044	2724.3	301.3	
13	1050	84.1 ± 5.6	0.032 ± 0.009	0.153 ± 0.006	9.671 ± 0.209	0.269 ± 0.042	2586.2	501.6	
14	1075	70.5 ± 5.5	0.029 ± 0.009	0.145 ± 0.005	13.649 ± 0.313	0.292 ± 0.043	2621.0	686.5	
15	1100	51.0 ± 5.4	0.025 ± 0.008	0.098 ± 0.003	7.452 ± 0.175	0.258 ± 0.042	2112.8	619.0	
16	1200	178.9 ± 5.6	0.067 ± 0.009	0.448 ± 0.008	19.023 ± 0.522	1.156 ± 0.063	2335.1	440.0	
17	1300	328.4 ± 13.8	0.072 ± 0.006	0.464 ± 0.010	9.914 ± 0.244	1.623 ± 0.097	2991.2	374.5	
18	1400	73.8 ± 13.4	0.016 ± 0.007	0.042 ± 0.005	0.684 ± 0.038	0.213 ± 0.086	3055.2	740.6	
19	1500	39.4 ± 14.5	0.014 ± 0.007	0.027 ± 0.007	0.347 ± 0.023	0.073 ± 0.093	2433.1	855.2	
17							213.6	15.3	

All isotope values are in 1e-8 ccSTP/g and ages are in Ma. This data has been blank corrected only.

Sample	Mass (mg)	J Factor	Split						
MB020f,2	13.47	1.062E-03	SB3						
Step #	Temp (°C)	⁴⁰ Ar	³⁹ Ar	³⁸ Ar	³⁷ Ar	³⁶ Ar	Apparent Age	± 2σ	
1	250	2011.1 ± 2.7	1.308 ± 0.012	1.103 ± 0.029	2.136 ± 0.024	5.475 ± 0.033	43.7	81.1	
2	300	587.3 ± 2.0	0.983 ± 0.011	0.303 ± 0.026	1.192 ± 0.024	1.334 ± 0.019	159.9	30.2	
3	350	418.6 ± 1.5	1.535 ± 0.013	0.233 ± 0.024	1.683 ± 0.058	0.920 ± 0.032	113.9	20.3	
4	400	231.8 ± 0.8	1.947 ± 0.015	0.147 ± 0.024	2.138 ± 0.044	0.393 ± 0.015	97.8	9.1	
5	450	164.4 ± 2.2	2.355 ± 0.015	0.135 ± 0.023	2.220 ± 0.070	0.255 ± 0.023	69.6	9.3	
6	500	230.8 ± 0.9	2.338 ± 0.020	0.195 ± 0.023	2.300 ± 0.050	0.397 ± 0.017	88.8	7.8	
7	550	104.5 ± 0.6	1.797 ± 0.015	0.094 ± 0.022	2.315 ± 0.050	0.207 ± 0.015	40.5	9.1	
8	600	93.0 ± 0.6	1.365 ± 0.012	0.071 ± 0.021	1.819 ± 0.028	0.207 ± 0.008	30.4	9.7	
9	650	103.8 ± 0.6	1.072 ± 0.012	0.075 ± 0.021	1.789 ± 0.034	0.090 ± 0.005	142.9	10.3	
10	700	116.9 ± 0.2	0.666 ± 0.009	0.076 ± 0.021	1.652 ± 0.032	0.155 ± 0.012	193.0	20.3	
11	750	153.5 ± 0.4	0.384 ± 0.009	0.067 ± 0.021	1.587 ± 0.031	0.160 ± 0.010	94.3	20.3	
12	800	188.3 ± 0.5	0.251 ± 0.006	0.061 ± 0.021	2.127 ± 0.066	0.183 ± 0.008	194.5	35.3	
13	1000	411.3 ± 0.6	0.302 ± 0.008	0.242 ± 0.023	11.953 ± 0.147	0.511 ± 0.014	99.3	75.0	
14	1200	526.5 ± 7.4	0.326 ± 0.007	1.045 ± 0.019	61.695 ± 0.367	3.484 ± 0.066	1856.8	35.6	
15	1400	296.7 ± 7.8	0.160 ± 0.004	0.905 ± 0.025	22.825 ± 0.191	3.783 ± 0.058	1858.0	51.6	
16	1500	37.7 ± 8.5	0.016 ± 0.005	0.007 ± 0.025	0.117 ± 0.030	0.044 ± 0.059	2206.8	460.6	
Total							169.3	7.3	

All isotope values are in 1e-8 ccSTP/g and ages are in Ma. This data has been blank corrected only.

Sample	Mass (mg)	J Factor	Split						
MB020f,5	9.32	1.062E-03	SB4						
Step #	Temp (°C)	⁴⁰ Ar	³⁹ Ar	³⁸ Ar	³⁷ Ar	³⁶ Ar	Apparent Age	± 2σ	
1	400	820.3 ± 6.2	1.210 ± 0.018	0.338 ± 0.018	1.335 ± 0.046	1.762 ± 0.061	422.4	30.1	
2	500	596.2 ± 5.2	1.597 ± 0.016	0.212 ± 0.015	1.849 ± 0.055	0.588 ± 0.053	463.5	18.2	
3	600	626.3 ± 5.0	1.484 ± 0.015	0.134 ± 0.015	2.582 ± 0.057	0.405 ± 0.041	566.4	15.5	
4	700	958.4 ± 5.0	1.137 ± 0.020	0.220 ± 0.015	2.332 ± 0.057	0.885 ± 0.048	913.7	22.4	
5	800	887.7 ± 5.1	0.770 ± 0.015	0.205 ± 0.016	2.491 ± 0.058	0.716 ± 0.042	1207.2	26.7	
6	900	1242.9 ± 5.3	0.714 ± 0.013	0.224 ± 0.015	4.159 ± 0.101	0.769 ± 0.077	1822.8	37.3	
7	925	1790.0 ± 5.4	0.695 ± 0.013	0.280 ± 0.016	4.581 ± 0.086	1.018 ± 0.048	2308.3	39.2	
8	950	2384.2 ± 6.2	0.741 ± 0.013	0.300 ± 0.016	5.475 ± 0.067	1.051 ± 0.041	2624.8	34.9	
9	975	2228.2 ± 5.8	0.665 ± 0.015	0.293 ± 0.015	6.924 ± 0.143	1.181 ± 0.042	2670.7	44.5	
10	1000	2293.9 ± 5.9	0.685 ± 0.014	0.396 ± 0.016	7.354 ± 0.125	1.358 ± 0.077	2663.6	44.3	
11	1025	2090.8 ± 4.1	0.608 ± 0.015	0.328 ± 0.024	7.114 ± 0.105	1.154 ± 0.080	2705.9	46.6	
12	1050	1625.1 ± 3.8	0.441 ± 0.013	0.286 ± 0.023	7.127 ± 0.177	1.275 ± 0.081	2771.9	63.9	
13	1075	989.7 ± 3.6	0.232 ± 0.011	0.178 ± 0.022	5.489 ± 0.118	0.808 ± 0.084	2980.6	86.9	
14	1100	465.4 ± 3.5	0.118 ± 0.008	0.148 ± 0.022	3.671 ± 0.070	0.698 ± 0.066	2767.6	241.6	
15	1200	1227.4 ± 3.6	0.356 ± 0.012	0.336 ± 0.023	5.427 ± 0.093	1.238 ± 0.075	2650.5	139.4	
16	1300	669.0 ± 22.6	0.177 ± 0.012	0.292 ± 0.022	4.576 ± 0.323	1.340 ± 0.084	2624.2	323.8	
17	1400	159.4 ± 21.9	0.056 ± 0.010	0.074 ± 0.019	1.740 ± 0.313	0.327 ± 0.076	2253.0	443.7	
18	1500	173.4 ± 23.8	0.070 ± 0.011	0.032 ± 0.020	1.491 ± 0.334	0.133 ± 0.080	2241.7	298.9	
Total							1730.5	15.9	

All isotope values are in 1e-8 ccSTP/g and ages are in Ma. This data has been blank corrected only.

Sample	Mass (mg)	J Factor	Split							
MB020f,5	9.96	1.061E-03	SBS	⁴⁰ Ar	³⁹ Ar	³⁸ Ar	³⁷ Ar	³⁶ Ar	Apparent Age	± 2σ
1	300	4536.8 ± 6.4	0.773 ± 0.015	2.709 ± 0.032	0.238 ± 0.066	14.636 ± 0.159	781.1	165.2		
2	400	744.4 ± 6.8	0.830 ± 0.017	0.330 ± 0.015	0.619 ± 0.064	1.373 ± 0.041	697.4	29.7		
3	450	472.9 ± 4.1	0.665 ± 0.015	0.086 ± 0.012	0.721 ± 0.064	0.360 ± 0.034	842.4	26.9		
4	500	654.9 ± 4.0	0.754 ± 0.013	0.189 ± 0.013	0.884 ± 0.063	0.815 ± 0.049	854.0	29.8		
5	600	954.3 ± 3.9	1.105 ± 0.015	0.134 ± 0.012	1.764 ± 0.066	0.427 ± 0.034	861.6	181.2		
6	700	1314.6 ± 4.2	1.151 ± 0.014	0.182 ± 0.015	2.611 ± 0.067	0.438 ± 0.034	1192.4	137.3		
7	750	948.4 ± 4.0	0.630 ± 0.012	0.168 ± 0.013	2.077 ± 0.072	0.669 ± 0.038	991.8	474.6		
8	800	979.6 ± 4.2	0.542 ± 0.012	0.106 ± 0.011	2.313 ± 0.068	0.456 ± 0.037	1440.7	301.0		
9	850	906.9 ± 4.1	0.391 ± 0.010	0.100 ± 0.012	2.493 ± 0.075	0.236 ± 0.032	2241.7	34.9		
10	900	1055.2 ± 4.2	0.474 ± 0.011	0.151 ± 0.012	3.266 ± 0.077	0.301 ± 0.032	2192.0	31.8		
11	950	2695.3 ± 4.9	0.829 ± 0.013	0.197 ± 0.015	6.389 ± 0.120	0.618 ± 0.032	2485.0	54.3		
12	1000	5293.0 ± 10.8	1.466 ± 0.017	0.416 ± 0.014	12.884 ± 0.230	1.179 ± 0.044	2641.5	49.8		
13	1050	7241.2 ± 5.9	1.879 ± 0.026	0.645 ± 0.016	19.280 ± 0.194	2.233 ± 0.055	2631.8	74.0		
14	1100	979.6 ± 4.2	0.542 ± 0.012	0.106 ± 0.011	2.313 ± 0.068	0.456 ± 0.037	2493.8	103.2		
15	1125	906.9 ± 4.1	0.391 ± 0.010	0.100 ± 0.012	2.493 ± 0.075	0.236 ± 0.032	2678.0	99.9		
16	1150	1055.2 ± 4.2	0.474 ± 0.011	0.151 ± 0.012	3.266 ± 0.077	0.301 ± 0.032	2534.1	179.9		
17	1175	2695.3 ± 4.9	0.829 ± 0.013	0.197 ± 0.015	6.389 ± 0.120	0.618 ± 0.032	2621.3	137.3		
18	1200	1075.1 ± 3.6	0.201 ± 0.014	0.204 ± 0.013	4.778 ± 0.072	0.735 ± 0.041	2604.1	255.0		
19	1225	683.4 ± 3.6	0.132 ± 0.014	0.182 ± 0.012	2.039 ± 0.069	0.635 ± 0.035	3344.5	169.4		
20	1250	450.5 ± 3.7	0.077 ± 0.013	0.189 ± 0.010	1.028 ± 0.060	0.678 ± 0.042	3492.3	135.0		
21	1300	483.6 ± 17.4	0.085 ± 0.014	0.193 ± 0.017	0.831 ± 0.093	1.304 ± 0.082	3380.4	289.8		
22	1350	117.5 ± 16.8	0.043 ± 0.013	0.041 ± 0.015	0.264 ± 0.086	0.195 ± 0.051	2375.3	454.4		
23	1400	124.2 ± 16.8	0.047 ± 0.014	0.038 ± 0.015	0.318 ± 0.086	0.197 ± 0.045	2346.1	429.2		
24	1500	76.8 ± 18.2	0.014 ± 0.014	0.039 ± 0.014	0.348 ± 0.093	0.150 ± 0.049	2479.0	1613.3		
Total							2035.0	29.4		

All isotope values are in 1e-8 ccSTP/g and ages are in Ma. This data has been blank corrected only.

Sample	Mass (mg)	J Factor	Split							
MB020f,5	10.30	1.056E-03	CH2							
Step #	Temp (°C)	⁴⁰ Ar	³⁹ Ar	³⁸ Ar	³⁷ Ar	³⁶ Ar	Apparent Age	± 2σ		
1	300	1696.8 ± 6.9	0.275 ± 0.018	1.084 ± 0.032	0.933 ± 0.198	7.325 ± 0.305	826.8	451.3		
2	400	546.3 ± 6.3	0.722 ± 0.017	0.197 ± 0.026	0.271 ± 0.172	1.057 ± 0.050	697.8	34.6		
3	450	406.6 ± 6.2	0.674 ± 0.018	0.037 ± 0.024	0.337 ± 0.169	0.356 ± 0.040	754.0	27.7		
4	500	532.6 ± 6.1	0.850 ± 0.020	0.097 ± 0.024	0.679 ± 0.168	0.558 ± 0.048	749.1	26.2		
5	550	485.9 ± 6.0	0.834 ± 0.022	0.035 ± 0.024	0.681 ± 0.167	0.123 ± 0.039	828.1	24.9		
6	600	509.2 ± 6.0	0.804 ± 0.018	0.049 ± 0.023	0.822 ± 0.167	0.120 ± 0.037	891.1	23.0		
7	650	644.5 ± 6.0	0.745 ± 0.021	0.056 ± 0.024	0.852 ± 0.165	0.198 ± 0.037	1114.9	28.6		
8	700	764.5 ± 6.0	0.750 ± 0.020	0.079 ± 0.023	1.014 ± 0.166	0.159 ± 0.038	1111.1	96.2		
9	750	863.9 ± 6.1	0.654 ± 0.017	0.057 ± 0.023	1.155 ± 0.166	0.231 ± 0.039	1197.7	130.5		
10	800	765.8 ± 6.1	0.519 ± 0.017	0.092 ± 0.023	1.263 ± 0.170	0.277 ± 0.039	1182.6	176.2		
11	850	895.5 ± 6.2	0.499 ± 0.020	0.094 ± 0.025	1.727 ± 0.176	0.394 ± 0.045	1151.4	255.1		
12	900	849.2 ± 6.3	0.432 ± 0.015	0.059 ± 0.025	1.992 ± 0.177	0.254 ± 0.040	1521.6	178.1		
13	925	825.0 ± 6.4	0.362 ± 0.015	0.029 ± 0.024	1.809 ± 0.179	0.152 ± 0.040	2211.1	54.8		
14	950	1049.1 ± 6.4	0.357 ± 0.016	0.067 ± 0.025	2.001 ± 0.183	0.150 ± 0.041	2550.6	64.4		
15	975	1369.2 ± 6.7	0.414 ± 0.018	0.084 ± 0.025	2.614 ± 0.186	0.234 ± 0.041	2534.0	83.9		
16	1000	1610.0 ± 6.7	0.469 ± 0.018	0.065 ± 0.026	3.141 ± 0.187	0.281 ± 0.045	2560.1	80.9		
17	1025	2574.4 ± 9.2	0.781 ± 0.024	0.158 ± 0.012	5.221 ± 0.186	0.569 ± 0.048	2456.5	72.5		
18	1050	3085.8 ± 9.1	0.897 ± 0.021	0.187 ± 0.014	6.654 ± 0.199	0.662 ± 0.053	2524.2	65.5		
19	1075	3085.8 ± 9.1	0.897 ± 0.021	0.187 ± 0.014	6.654 ± 0.199	0.662 ± 0.053	2461.9	74.7		
20	1100	4302.8 ± 9.1	1.240 ± 0.026	0.314 ± 0.017	10.502 ± 0.234	1.168 ± 0.052	2514.0	98.5		
21	1150	3058.0 ± 9.0	0.801 ± 0.020	0.269 ± 0.015	8.311 ± 0.189	1.008 ± 0.060	2434.5	170.1		
22	1200	4315.8 ± 9.4	1.109 ± 0.023	0.812 ± 0.019	12.606 ± 0.194	4.296 ± 0.094	2585.2	179.6		
23	1300	13342.9 ± 14.6	3.845 ± 0.039	1.992 ± 0.035	45.605 ± 0.552	10.465 ± 0.164	2511.8	130.5		
24	1400	3358.2 ± 10.6	0.977 ± 0.023	0.676 ± 0.021	9.495 ± 0.212	2.832 ± 0.083	2485.9	139.2		
25	1500	288.2 ± 12.1	0.133 ± 0.016	0.053 ± 0.017	0.446 ± 0.205	0.470 ± 0.048	2144.4	162.5		
Total							2047.1	42.1		

All isotope values are in 1e-8 ccSTP/g and ages are in Ma. This data has been blank corrected only.